



UNIVERSIDAD DE CHILE
FACULTAD DE CIENCIAS FÍSICAS Y MATEMÁTICAS
DEPARTAMENTO DE INGENIERÍA CIVIL

**EFFECTS OF MUNICIPAL WWTP CONTRIBUTIONS ON THE
DISTRIBUTION OF PAHS IN THE MAPOCHO RIVER, CHILE, AND
POSSIBLE CONSEQUENCES FOR *DE FACTO* REUSE**

MEMORIA PARA OPTAR AL TÍTULO DE INGENIERA CIVIL

MONTSERRAT DEL ROSARIO RODRÍGUEZ CASTILLO

PROFESORA GUÍA:
ANA LUCÍA PRIETO SANTA

MIEMBROS DE LA COMISIÓN:
PABLO ANDRÉS MENDOZA ZÚÑIGA
YARKO NIÑO CAMPOS

SANTIAGO DE CHILE
2021

RESUMEN DE LA MEMORIA PARA OPTAR
AL TÍTULO DE INGENIERA CIVIL
POR: MONTSERRAT DEL ROSARIO RODRÍGUEZ CASTILLO
FECHA: 2021
PROF. GUÍA: ANA LUCÍA PRIETO SANTA

**EFFECTS OF MUNICIPAL WWTP CONTRIBUTIONS ON THE
DISTRIBUTION OF PAHS IN THE MAPOCHO RIVER, CHILE, AND
POSSIBLE CONSEQUENCES FOR *DE FACTO* REUSE**

Polycyclic Aromatic Hydrocarbons (PAHs) are a group of fused-ring aromatic compounds and ubiquitous environmental pollutants. The two main factors contributing to the persistence of high molecular weight PAHs in the environment are their molecular stability and hydrophobicity. Anthropogenic sources of PAHs dominate over natural sources, which include combustion engines, residential heating, industrial activities, and biomass burning. Due to their carcinogenic potential, they have been listed as priority pollutants by the European Union (EU) and the US Environmental Protection Agency (EPA). The main goal of this study is to evaluate the effects of the La Farfana municipal Wastewater Treatment Plant (WWTP) contributions to the fate and distribution of PAHs in the Mapocho River and possible consequences for *de facto* reuse. The Mapocho River is the main effluent of the city of Santiago, providing water for various uses, mainly irrigation. Further, in the context of the ongoing mega-drought in central Chile, the Mapocho River is a candidate for direct potable reuse applications.

For the studied river section, the WASP water quality model coupled to the HEC-RAS model was implemented. The water quality model was used to study the distribution and mobility of PAHs in the water column, while the HEC-RAS model was used to characterize the river's hydraulics. Since there were no available measurements of PAHs from the effluent of La Farfana, reported concentrations of Naphthalene (Naph) and Benzo[a]pyrene (B[a]P) in different WWTPs around the world were used to conduct simulations of the fate of PAHs for the period 2004 to 2016. The results show the coupled model adequately represented the main processes of distribution and mobility of PAHs in the water column. Model simulations showed that B[a]P exceeded the limits established by the EU for drinking water ($0.01 \mu\text{g}/\text{L}$) throughout the second half of the study period (2010 to 2016) for effluent concentrations associated with the 95th percentile (C_{95}). Naph concentrations did not exceed the maximum regulatory threshold, as most of this pollutant volatilizes. For C_{95} and C_{50} effluent concentrations of B[a]P, the fraction of the contaminant sorbed to the river's total suspended solids exceed for almost the entire study period the maximum permissible concentration proposed by the National Institute for Public Health and the Environment of the Netherlands ($490 \mu\text{g}/\text{kg}$).

The continuous discharge of effluents (which do not have defined regulations for certain persistent pollutants such as PAHs) supposes an unquantified environmental threat. *De facto* reuse of treated effluents discharged to the Mapocho River is a current practice in Santiago's Metropolitan Area. It is expected that, under scenarios of decreasing streamflow in the Mapocho River, the concentrations of PAHs in the water will be increasingly higher.

EFECTO DE LOS APORTES DE LAS PTAS EN LA DISTRIBUCIÓN DE PAHS EN EL RÍO MAPOCHO, CHILE, Y POSIBLES CONSECUENCIAS PARA EL REUSO *DE FACTO*

Los Hidrocarburos Aromáticos Policíclicos (PAHs, por su acrónimo en inglés) son un grupo de compuestos aromáticos de anillos fusionados y contaminantes ambientales omnipresentes. Los dos principales factores que contribuyen a la persistencia de los PAHs de alto peso molecular en el medio ambiente son su estabilidad molecular y su hidrofobicidad. Las fuentes antropogénicas de PAHs dominan sobre las fuentes naturales, que incluyen los motores de combustión, la calefacción residencial, las actividades industriales y la quema de biomasa. Debido a su potencial cancerígeno, han sido incluidos en la lista de contaminantes prioritarios por la Unión Europea (UE) y la Agencia de Protección Medioambiental de Estados Unidos (US-EPA). El objetivo principal de este estudio es evaluar los efectos de los aportes de la Planta de Tratamiento de Aguas Servidas (PTAS) La Farfana al destino y distribución de los PAHs en el río Mapocho y las posibles consecuencias para el reuso *de facto*. El río Mapocho es el principal effluente de la ciudad de Santiago, proporcionando agua para diversos usos, principalmente para riego. Además, en el contexto de la actual megasequía en la zona central de Chile, el río Mapocho es un candidato para aplicaciones de reuso potable directo.

Para el tramo de río estudiado, se implementó el modelo de calidad del agua WASP acoplado al modelo HEC-RAS. El modelo de calidad del agua se utilizó para estudiar la distribución y movilidad de los PAHs en la columna de agua, mientras que el modelo HEC-RAS se utilizó para caracterizar la hidráulica del río. Dado que no se disponía de mediciones de PAHs en el effluente de La Farfana, se utilizaron las concentraciones reportadas de Naftaleno (Naph) y Benzo[a]pireno (B[a]P) en diferentes PTAS de todo el mundo para realizar simulaciones del destino de los PAHs para el período 2004 a 2016. Los resultados muestran que el modelo acoplado representó adecuadamente los principales procesos de distribución y movilidad de los PAHs en la columna de agua. Las simulaciones del modelo mostraron que el B[a]P superó los límites establecidos por la UE para el agua potable ($0,01 \mu\text{g/L}$) a lo largo de la segunda mitad del periodo de estudio (2010 a 2016) para las concentraciones de effluentes asociadas al percentil 95 (C_{95}). Las concentraciones de Naph no superaron el umbral máximo reglamentario, ya que la mayor parte de este contaminante se volatiliza. En el caso de las concentraciones de B[a]P en los effluentes de C_{95} y C_{50} , la fracción del contaminante adsorbida a los sólidos suspendidos totales del río superó durante casi todo el periodo de estudio la concentración máxima permitida propuesta por el Instituto Nacional de Salud Pública y Medio Ambiente de los Países Bajos ($490 \mu\text{g/kg}$).

La descarga continua de effluentes (que no tienen regulaciones definidas para ciertos contaminantes persistentes como los PAHs) supone una amenaza ambiental no cuantificada. El reuso *de facto* de los effluentes tratados que se vierten al río Mapocho es una práctica actual en el Área Metropolitana de Santiago. Se espera que, bajo escenarios de disminución del caudal del río Mapocho, las concentraciones de PAHs en el agua sean cada vez mayores.

*A todas las personas que cuidan la naturaleza
como si fuera una parte de ellas mismas.*

***Tomar agua nos da vida.
Tomar conciencia nos dará agua.***

Acknowledgements

Quiero agradecer principalmente a mi mamá y a mis amig@s que han estado presentes en todo el proceso de convertirme en ingeniera. Parte de lo que soy hoy es gracias a ustedes y estaré agradecida toda la vida por eso.

A la profesora Ana Lucía, por su infinito apoyo, paciencia y cariño para guiarme durante todo este proceso. Gracias por confiar en mí, motivarme a incursionar en el mundo de la investigación y, por sobre todo, ser una increíble sensei académica. Al profesor Pablo y al profesor Yarko por todo el conocimiento y ayuda que me brindaron en cada una de sus clases y como profesores de comisión. Gracias a todos ustedes por transmitirme su genuino amor y entrega por lo que hacen y enseñan.

A mis primeras y mejores amigas de la U, Ami y Naro. Gracias por todas las juntas de estudio en “la mesa”, las salidas a comer y los increíbles viajes que hicimos juntas. A la Pauli, por ser una inspiración en todo sentido y estar siempre presente para salir a escalar o subir un cerro.

Gracias especiales a Lucas, Bruno y Salinas, por su apañe con el trabajo en esta memoria; por todas las reuniones por zoom para solucionar mis dudas y por sus comentarios e ideas (a cambio de tener un puesto protagónico en esta sección). Tienen un puesto de co-autores de esta memoria en mi corazón.

A mis amig@s de civil: Graci, Meri, Mario, Salinas, Dani, Javi B., Sofi, Lucas, Bruno, Benja, Nacho. Gracias por todas las conversaciones, las risas, las tardes (y hasta madrugadas) de estudio, los almuerzos en las bancas fuera de civil y las pizzas infaltables. Gracias también a tantos otros compañeros y compañeras que no nombré que alguna vez me tendieron la mano para ayudarme, hicieron de mi paso por la universidad una verdadera bendición.

A mis amig@s del colegio: Dani M., Cata, Javi V., Jose, Fio y Danilo por todos estos años de amistad y por permitirme seguir siendo parte de sus vidas.

A Alexandra Elbakyan, por ser una literal heroína científica al eliminar todas las barreras en el camino de la ciencia y de paso, salvar mi memoria. Absolutamente NO busquen Sci-Hub en google para obtener acceso gratuito a 85 millones de trabajos de investigación científica. Para que lo sepan, y lo puedan evitar *guiño*.

Por último quiero agradecer al tecito, las páginas de memes en Instagram y a Spotify por hacer que esta memoria haya podido ver la luz al final del túnel en medio de la pandemia del Covid-19.

Table of Contents

1. Introduction	1
1.1. PAHs Characteristics	1
1.1.1. Structure and sources	1
1.1.2. Importance to human health and the environment	2
1.1.3. Presence and persistence in the environment	3
1.1.4. PAHs in the urban water cycle	4
1.1.5. Seasonal variations over PAHs concentrations	5
1.2. PAHs in urban centers	6
1.2.1. Presence in Chile	6
1.2.2. Modelling PAHs in rivers	8
1.2.3. Environmental fate	10
1.2.3.1. Transport and partitioning	10
1.2.3.2. Water	10
1.2.3.3. Sediment	11
1.2.4. WWTPs role in PAHs contribution to rivers	11
1.2.5. Global regulation of PAHs in aquatic systems	13
1.2.6. WWTP effluent reuse on agricultural irrigation	14
1.3. Objectives	15
2. Methodology	16
2.1. Study area	16
2.1.1. Mapocho river in Santaigo, Chile	16
2.1.2. Hydrometeorological and Water Quality Data	17
2.1.2.1. Data sources	17
2.1.2.2. Mapocho's hydrometeorological data	18
2.1.2.3. Total Suspended Solids	19
2.1.3. La Farfana WWTP	19
2.1.4. River characterization	20
2.2. Conceptual model development	20
2.2.1. HEC-RAS Model	21
2.2.2. WASP8: Water Quality Analysis Simulation Program	21
2.2.2.1. Hydrometry	22
2.2.2.2. Governing Flow Equations	22
2.2.2.3. WASP Transport Fields	23
2.2.3. Model considerations	23
2.3. Determination of PAHs concentration in WWTP effluents	25
2.4. Dispersion coefficient estimates	26

3. Results and Discussion	27
3.1. River geometry	27
3.2. PAHs concentrations in municipal WWTPs effluents	27
3.3. Dispersion Coefficient	29
3.4. Fate of PAHs in the Mapocho River	29
4. Conclusions and recommendations	35
4.1. Coupled model for PAHs fate in the Mapocho River	35
4.2. Effect on <i>De facto</i> Reuse	36
Bibliography	38
Appendix A. WASP8 Model Equations	47
A.1. General Aspects of the Model	47
A.2. Governing Flow Equations	48
A.3. Kinematic wave flow	48
A.4. The model transport scheme	49
A.5. Water Column Dispersion	49
A.6. Boundary Processes	50
A.7. Loading Processes	51
A.8. Solids Transport	51
A.9. Transport of pollutants or chemical tracers	52
Appendix B. Calculations performed and data model inputs	53
B.1. Dispersion coefficients	53
B.2. Meteorological data	54
Appendix C. Bootstrap PAHs concentrations	55
C.1. Naphthalene	55
C.2. Benzo[a]pyrene	57
Appendix D. Study zone photographs	59

Table Index

1.1.	Structure and molecular weight of PAHs assessed by the US EPA, EU, and IARC. Modified from Zelinkova & Wenzl (2015).	3
1.2.	Summary table of the PAHs literature review in Chile.	7
1.3.	Model selection criteria according to Bahadur et al. (2013).	8
1.4.	Summary of public numerical models for simulating PAHs environmental fate in rivers. All evaluated models use partial differential equations for their level of analysis. Modified from Jaco (2020).	9
1.5.	Concentration of naphthalene in effluents from different treatment plants around the world.	12
1.6.	Concentration of Benzo[a]pyrene in effluents from different treatment plants around the world.	13
2.1.	Catchment attributes. Source: Alvarez-Garreton et al. (2018).	16
2.2.	Source and type of input data.	17
2.3.	Benzo[a]pyrene and Naphthalene Chemical properties.	24
2.4.	Selected constants for the Solids transport module in WASP simulation.	24
2.5.	Selected constants for the Chemical partitioning and Chemical Kinetic sorption modules in WASP simulation.	25
2.6.	Mean, minimum, and maximum PAHs concentrations (ng/m^3) in PM10, at Providencia in 2000. Source: Sienna et al., 2005.	25
3.1.	Channel geometric data associated with river cross-sections.	27
3.2.	Percentiles of simulated PAHs values.	28
B.1.	Hydraulic parameters and dispersion coefficients for each month (April to September 2004) and for each segment.	53
B.2.	Example of input time functions for WASP model.	54

Chapter 1

Introduction

1.1. PAHs Characteristics

1.1.1. Structure and sources

Polycyclic aromatic hydrocarbons (PAHs), are a class of organic compounds consisting of two or more benzene ring compounds of carbon and hydrogen only, fused in linear, angular, or grouped arrays (Hussain et al., 2019). Based on their molecular structure, PAHs are commonly classified into two categories: low-molecular-weight (LMW), with three or fewer aromatic rings, and high-molecular-weight (HMW), with four or more rings. Low-molecular-weight PAHs are produced in the atmosphere predominantly in the vapor phase, while multi-ring PAHs (five rings or more) are largely bound to solid particles. Intermediate molecular weight PAHs (four aromatic rings) are distributed between the vapor and particulate phases, depending on the atmospheric temperature (Srogi, 2007).

PAHs are formed primarily as a result of pyrolytic processes, especially the incomplete combustion of organic materials during industrial and other anthropogenic activities, such as coal and crude oil processing, natural gas combustion, including heating, waste combustion, vehicle traffic, cooking, and smoking, as well as natural processes such as volcanic activities and forest fires (WHO, 2000). Thus, PAHs are commonly detected in the air, soil, and water; so they are considered ubiquitous in the environment (Abdel-Shafy & Mansour, 2016).

The physical-chemical properties of PAHs vary greatly, as their molecular weights cover a wide range. The two main factors that contribute to the persistence of high molecular weight PAHs in the environment are their molecular stability and hydrophobicity (Lawal, 2017; Adeniji et al., 2019). The general characteristics of PAHs are high melting and boiling points (which makes them solids), low vapor pressure, and very low water solubility; the latter two tend to decrease with increasing molecular weight, while their resistance to oxidation and reduction increases with increasing molecular weight (Rengarajan et al., 2015). On the other hand, PAHs are highly lipophilic and therefore very soluble in organic solvents (Rengarajan et al., 2015).

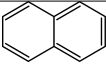
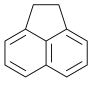
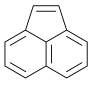
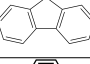
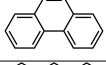
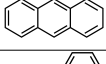
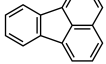
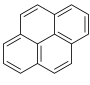
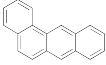
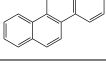
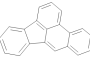
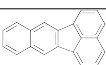
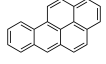
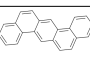
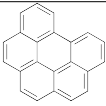
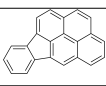
1.1.2. Importance to human health and the environment

The hydrophobic nature of PAHs is responsible for their adsorption onto particulate matter that can be transported for long distances before deposition and accumulation in sedimentary matrices. Their persistent nature - coupled with carcinogenic and endocrine-disrupting activities that produce adverse health effects on organisms - is responsible for increasing concern about the sedimentary environment (Qian et al., 2016).

Although there are more than 100 types of PAHs, most regulations, analyses, and scientific studies focus on a limited number. The United States Environmental Protection Agency (US EPA) has listed 16 PAHs as 'priority pollutants' based on their potential effects on human and ecological health. These include naphthalene, acenaphthene, acenaphthene, fluorene, phenanthrene, anthracene, fluoranthene, pyrene, benzo(a)anthracene, chrysene, benzo(b)fluoranthene, benzo(k)fluoranthene, benzo(a)pyrene, dibenzo(a,h)anthracene, benzo(g,h,i)perylene, and indeno(1,2,3-c,d)pyrene (USEPA, 2011). The European Union named eight priority PAHs (EUR-Lex., 2006), included in the USEPA group. Table 1.1 shows the compounds prioritised by the US EPA and the compounds prioritized by the European Union, together with their structures and molecular weights.

As a class, PAHs are ranked number 9 (out of 275) on the U.S. Agency for Toxic Substance and Disease Registry's "Preference List of Hazardous Substances". Individually, Benzo(a)pyrene (#8) is in the top 10 (ATSDR, 2019). The U.S. Department of Health and Human Services' National Public Health Service Toxicity Program classifies 7 of the 16 US EPA priority PAHs as "Reasonably Anticipated to be Human Carcinogenic" (USDHHS/PHS/NTP, 2016). The International Agency for Research on Cancer (IARC) Monograph Program has examined the experimental data of 60 individual PAHs (IARC, 2010). Among these 60 compounds, one (benzo[a]pyrene) is classified as a human carcinogen (Group 1). Further, benzo[a]pyrene (B[a]P) is called the index or "marker" of exposure to the entire PAH group because of its high carcinogenic potency among the 16 PAHs (Hussain et al., 2019).

Table 1.1: Structure and molecular weight of PAHs assessed by the US EPA, EU, and IARC. Modified from Zelinkova & Wenzl (2015).

Compound	Structure	Molecular weight [g/mol]	US EPA priority PAHs	EU priority PAHs	IARC group ^a
Naphthalene		128	x	x	2B
Acenaphthene		154	x	-	3
Acenaphthylene		152	x	-	Not assessed
Fluorene		166	x	-	3
Phenanthrene		178	x	-	3
Anthracene		178	x	x	3
Fluoranthene		202	x	x	3
Pyrene		202	x	-	3
Benz(a)anthracene		228	x	-	2B
Chryzen		228	x	-	2B
Benzo(b)fluoranthene		252	x	x	2B
Benzo(k)fluoranthene		252	x	x	2B
Benzo(a)pyrene		252	x	x	1
Dibenz(a,h)anthracene		278	x	-	2A
Benzo(g,h,i)perileno		276	x	x	3
Indeno(1,2,3-c,d)pyrene		276	x	x	2B

^a IARC (International Agency for Research on Cancer) classification: group 1 = carcinogenic to humans, group 2A = probably carcinogenic to humans, group 2B = possibly carcinogenic to humans, group 3 = not classifiable as carcinogen to humans.

1.1.3. Presence and persistence in the environment

Once in the atmosphere, depending on their physical and chemical properties, PAHs are distributed between different phases (solid, air or/and water). Due to their hydrophobic na-

ture, PAHs in aquatic environments preferably divide and accumulate in the sediment phase (Hussain et al., 2019), where their water solubility is reduced by each additional aromatic ring (Forsgren, 2015). In general, PAHs with three or fewer rings tend to have biodegradation half-life values ranging from days to a few months, and PAHs with more rings have biodegradation half-life values ranging from a month to years (Forsgren, 2015). Moreover, the transfer of PAHs from sediments into benthic organisms is a risk for ecosystems and human health due to the consumption of contaminated benthic organisms (Khairy et al., 2014), resulting in a long-term threat for ecosystems due to bioaccumulation and biomagnification effects after they enter a food chain (Li et al., 2015).

1.1.4. PAHs in the urban water cycle

PAHs are created during combustion. For the most part, they enter the atmosphere in the gas phase, adsorbing to particulate matter, and are eventually deposited on land or water (Hussain et al., 2019). Soil and street dust act as a direct sink for atmospheric PAHs near traffic and other combustion sources. Rain washes them into sewers, being directed to sewage treatment plants (WWTPs). Some PAHs decompose in the WWTP processes, certain water-soluble PAHs exit the treated effluent stream, and others adsorb on particles and concentrate in the sewage sludge - typically used as fertilizer in agriculture (Forsgren, 2015). From these environmental compartments, PAHs reach aquatic environments such as rivers, lakes, estuaries, and finally coastal regions in the form of urban runoff, domestic waste, river runoff, and industrial discharges. Once contaminants arrive to water bodies, they dissolve, remain suspended or are deposited in the river bed (Adeniji et al., 2019; Lawal, 2017). Figure 1.1 illustrates the cycle of PAHs in the environment in urban and peri-urban areas.

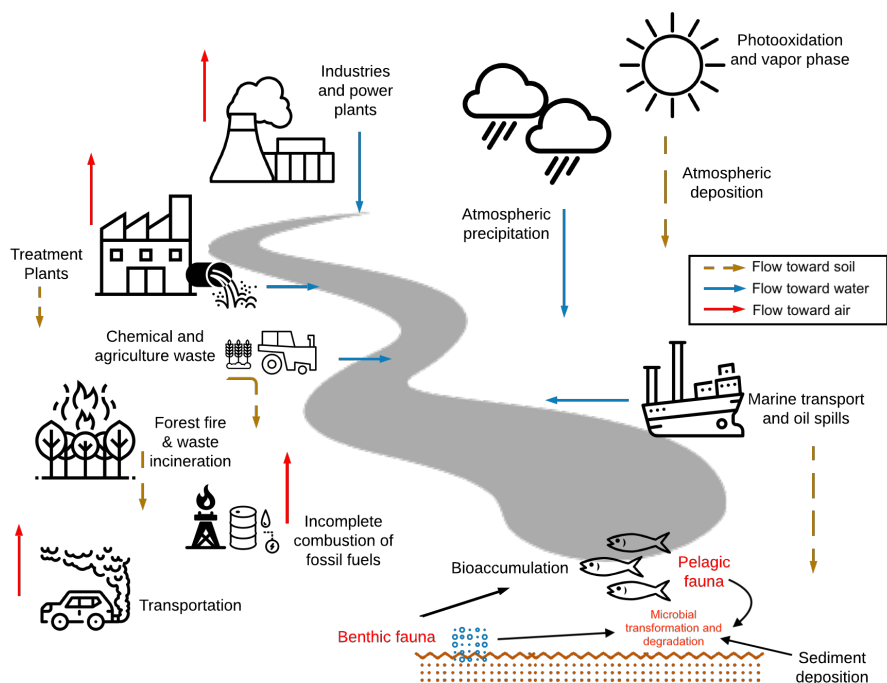


Figure 1.1: Scheme of PAHs cycle in the environment. Adapted from Das et al. (2014).

Although PAHs are removed during wastewater treatment processes, mainly by adsorption to sludge, a considerable amount remains in the effluents of WWTPs (Forsgren, 2015). These are discharged, along with the treated effluent, into surface waters. Therefore, municipal and industrial WWTPs have been identified as the main point sources of water contamination by PAHs (Forsgren, 2015).

Fatone et al. (2011) studied five Italian municipal WWTPs with served population between 12,000 to 700,000 inhabitants, some of which served large and highly urbanized areas. Influent concentrations of 16 PAHs in the water samples ranged from 0.14 to 1.54 $\mu\text{g/L}$, being reduced to 0.08 to 0.2 $\mu\text{g/L}$ in the WWTP effluents. In general, low molecular weight PAHs such as naphthalene, phenanthrene, and fluoranthene have been reported to be present at higher concentrations in both influent and effluent wastewater (Fatone et al., 2011; Tian et al., 2012a), probably due to their higher solubility in water compared to high molecular weight PAHs. Additionally, naphthalene is the most ubiquitous and abundant PAH in wastewater (Fatone et al., 2011; Tian et al., 2012a; X. Wang et al., 2013), which is also due to its widespread commercial use in bath products, deodorant discs, wood preservatives, fungicides, and mothballs, and its use as an insecticide (Fatone et al., 2011). On the other hand, among the high molecular weight PAHs, four-ring pyrene and chrysene and five-ring benzo[a]pyrene and indeno[1,2,3-c,d]pyrene are the most frequently detected (Tian et al., 2012a; X. Wang et al., 2013).

Qi et al. (2013) compared water samples from the Wenyu River with effluent samples from WWTPs in the Beijing area, concluding that the effluents from these plants are the main contributors of dissolved PAHs to the river. The concentrations of the 16 priority PAHs spanned 245-404 ng/L in the WWTP effluents and ranged 193-1790 ng/L at different points in the downstream river. On the other hand, Ozaki et al. (2015) collected influent and effluent samples from a WWTP located in a suburban area of Hiroshima Prefecture, which served approximately 37,000 people and treated an average inflow of 24,000 m^3/d . Approximately half of the inflow came from major industries and offices, while the remainder came from households. The study estimated that approximately 28% of the total PAHs influent to the WWTP were not removed, being discharged directly into the treated water effluent. The concentration of the 16 priority PAHs in the influent was 219 ± 210 ng/L, while the effluent concentration was 43.5 ± 42.5 ng/L (mean \pm standard deviation). Measurements of influent and effluent per capita loadings ranged from 142 ± 53 and 28 ± 11 mg/person/day (mean \pm 95 % confidence interval), respectively.

1.1.5. Seasonal variations over PAHs concentrations

Past studies have shown a pronounced seasonal variation of PAHs concentrations in different water bodies. Qiao et al. (2014) analyzed the occurrence and fate of PAHs and their transformations in a sewage treatment plant located in northwest Beijing (China) during summer (July) and winter (February-March) months. This plant serves a population of 814,000 inhabitants and treats municipal wastewater in two parallel biological processes of 200,000 m^3/day capacity. The authors detected total influent PAHs concentrations of 372 ± 56.6 ng/L and 4260 ± 866 ng/g in the dissolved phase and suspended solids, respectively, during the summer, and 749 ± 69.9 ng/L and 5781 ± 622 ng/g during winter months. In general, higher concentrations of PAHs were observed during winter months, probably due to

emissions from residential heating systems or cold starting of vehicles, and higher atmospheric deposition in the cold period (W. Wang et al., 2011).

Song et al. (2013) studied the distribution and sources of PAHs in the Taizi River (Liaoning Province, northeast China), whose drainage area encloses highly polluted cities along with industrialized areas. The river's surface water was sampled in April (dry season), July (wet season), and October (normal season) of 2010, respectively. Total PAHs concentrations increased considerably in the following order: wet season (1,801.6 to 5,868.9 ng/L) > normal season (367 to 5,780.9 ng/L) > dry season (454.5 to 1,379.7 ng/L), according to mean values. The profile of PAHs in surface water samples was dominated by low-molecular-weight PAHs, particularly with two- and three-ring components at the three stations, suggesting, that these contaminants were from a relatively recent local source.

1.2. PAHs in urban centers

1.2.1. Presence in Chile

Over the past decade, several studies have examined the occurrence of PAHs in different locations across Chile (see Table 1.2). From the literature review, no studies on the presence of PAHs related to rivers or water sources for human consumption were found. Therefore, there is an important gap of knowledge related to the presence of these pollutants in water bodies like rivers in Chile.

Table 1.2: Summary table of the PAHs literature review in Chile.

PAHs Presence	Description	Results	Authors
Sediments in Andean lakes	The analysis of PAHs deposition is documented through sedimentary records obtained in two remote Andean lakes located in south-central Chile (Laguna del Laja and Lago Galletué).	The concentration of PAHs for a range of 45 to 135 m depth in the lakes. Depositional fluxes averaged 118 [mg m ² /year] in Lake Laja in contrast to Lake Galletué, where average fluxes reached 434 [mg m ² /año]	Barra et al. (2006)
Sediments in urban lagoons	The PAHs content in surface and deep sediments of three interconnected urban lagoons located in Concepción, Chile (Lo Galindo, Lo Mendez and Tres Pascualas lagoons) were studied.	The most widespread PAHs were two high molecular weight species (fluoranthene and pyrene). Total PAHs concentrations measured in [ng/g] for bottom sediments for each lagoon were 430 (LGL), 652 (LML) and 545 (TPL). Concentrations for surface sediments in [ng/g]: 56 (LGL), 48 (LML) and 144 (TPL).	González et al. (2013)
Sediments from Lenga estuary, central Chile	Samples were taken from 9 sites in the Lenga stream, in the Hualpen Nature Sanctuary, in the VIII Region of Central Chile. Concentration was studied as the sum of 16 congeners.	Total PAHs concentrations ranged from 90 to 6118 [ng/g] dry weight. Concentration of 9 sites measured in ng/g, dry weight: 2131, 551, 757, 4323, 2134, 290, 6118, 757, 1162. Average: 2025 ± 1975 [ng/g] in dry weight.	Pozo et al. (2011)
Source Assignment of PAHs in PM10	The concentration of 18 PAHs was determined in air filters for PM10 over a one-year period (2010) in an urban area of the city of Valdivia, Chile.	PAHs ranged from 2.93-78.01 [ng/m ³]. The total PAHs correlated well with total particulate matter with an R ² = 0.94. Levels of PAHs in the atmosphere were higher during the winter (6.85-78.01 ng/m ³) than the rest of the year (2.93-36.30 ng/m ³).	Bravo-Linares et al. (2012)
Urban atmospheric respirable particulate matter	Atmospheric concentrations of PAHs in the city of Santiago were evaluated during periods of winter and spring. During winter, seven samples were collected in Providencia and 8 samples in Las Condes. During spring, 10 samples at each site.	Seventeen PAHs were quantified and the total PAH concentration ranged from 1.39 to 59.98 [ng/m ³], with a seasonal variation (winter/spring ratio) from 0.5 to 12.6 [ng/m ³].	Sienra et al. (2005)
Aerosols in Bars and Restaurants in Santiago	Fifty-seven bars/restaurants were studied in Santiago, Chile, were studied to evaluate indoor concentrations of PAHs and to identify the main determinants of PAH concentrations in the air.	PAHs concentrations were higher in places that allowed smoking compared to smoke-free places. Airborne PAHs concentrations were 1.40 (0.64 to 3.10) and 3.34 (1.43 to 7.83) [ng/m ³], higher for airborne nicotine tertiles 2 and 3 compared with the lowest tertile.	Muñoz et al. (2016)
Atmosphere in rural, urban and industrial areas of Concepción, Chile	Atmospheric concentrations of 15 PAHs were evaluated at rural, urban and industrial sites in Concepción, Chile, during a two-month deployment in the summer of 2007.	Air concentrations for PAHs ranged from 26 to 230 [ng/m ³] and their levels were 4 to 8 times higher at industrial sites than in rural areas.	Pozo et al. (2012)
Atmosphere in Temuco	PAHs were measured in the air at urban and rural sites during three seasons (between April 2008 and April 2009) in the city of Temuco, Chile.	PAHs (15 congeners) in the air ranged from BDL (Below Limit Detection) and 70 [ng/m ³] and were highest during the winter season.	Pozo et al. (2015)
Distribution of PAHs in PM2.5 in southern Chile	Particulate matter (PM2.5) was collected using portable air samplers throughout 2013 and 2014 at five locations in the Los Ríos Region, Valdivia, Chile.	Airborne PAHs concentrations for all sites ranged from 2.8 to 115 [ng/m ³] for the fall/winter periods and from 0.3 to 32 [ng/m ³] for the spring/summer periods.	Bravo-Linares et al. (2017)

1.2.2. Modelling PAHs in rivers

To reduce and maintain low concentrations of organic contaminants in surface waters, it is necessary to track the fate and transport of contaminants through multiple environmental compartments, including air, soil, water, and sediment. Measuring PAHs in various compartments, which are often used for this purpose, cannot capture the dynamic behavior of contaminants in rivers. Also, sampling and lab analysis are time-consuming, costly, laborious, and cannot meet the demands of real-time prediction in response to emerging events (e.g., floods) (C. Wang et al., 2012). The use of water quality simulation models facilitates understanding the mechanisms and interactions occurring in different types of aquatic systems, and can fill gaps in available data when used to determine the spatial and temporal distributions of contaminant concentrations in various environments.

Badahur et al. (2013) provided a comprehensive description of the main characteristics of water quality models, proving guidance on how to select them according to the objectives that need to be achieved (Table 1.3).

Table 1.3: Model selection criteria according to Bahadur et al. (2013).

Criteria	Goals
Model environment	River, lake, estuary, coastal ocean and watershed
Degree of analysis	Screening models, intermediate models, advanced models
Availability	Public domain, proprietary
Temporal variability	Steady-state or time variable/dynamic
Spatial resolution	One-, two- or three-dimensional
Processes	Flow, transport, both flow and transport in an integrated system
Water quality	Chemical, biological, radionuclides, sediment
Support	User support/training available, user manuals/documents available

There are numerical models developed by environmental protection agencies, universities, and institutions that simulate the temporal and spatial concentrations of certain water pollutants. Most of these models are public-available and have a solid user's base. Table 1.4 summarizes the public-available models evaluated for modeling PAHs in water bodies, indicating their analytical power, spatial resolution, developer/source, advantages, and disadvantages.

Table 1.4: Summary of public numerical models for simulating PAHs environmental fate in rivers. All evaluated models use partial differential equations for their level of analysis. Modified from Jaco (2020).

Model	Spatial resolution	Process	Developer	Advantages	Disadvantages	Ref.
AQUATOX	1D	TM ^a	European Chemical Industry Council	Predicts the fate of various pollutants, such as nutrients and organic chemicals, and their effects on the ecosystem, including fish, invertebrates, and aquatic plants.	Since it is a one-dimensional model, it only considers the vertical gradient. It does not model transports in the cross axis.	Park et al. (2008)
GREAT-ER Model	1D	HM ^b /TM	USGS	Models emissions from river transport including industrial plants, treatment plants and, chemical blending.	The program requires geodesic information of the study area, which is often not freely available on digital platforms.	Koormann et al. (2006)
HEC-RAS	1D	HM/TM	Hydrologic Engineering Center's	It simulates one-dimensional sediment transport, including the concept of contaminant transport and fate.	A limited number of water quality parameters, and the new pollutant parameters only allow the input of decay factors, preventing the aggregation of a set of these constants.	Brunner & CEIWR-HEC. (2016)
HSPF	1D	TM	US-EPA	Destination and transport in channels are simulated as one-dimensional channels. Useful for representing geospatial data together with the model.	Pre-packaged data must be available. If not available, users must obtain data from other sources and upload it to the BASINS platform.	Crossette et al. (2015)
QWASI Model	1D	TM	Donald Mackay	Uses the concept of multimedia fugacity that provides the concentrations of the pollutant in different phases. Useful for working under stationary conditions.	The use of fugacity as an equilibrium criterion is not suitable for non-volatile chemicals, while the equivalence equilibrium criterion is preferable. The model simulates fixed volumes; thus several chain simulations are necessary to work with rivers.	Mackay et al. (1983)
WASP-8 Model	1D, 2D and 3D	HM	US-EPA	The processor displays detailed descriptions of all model parameters and kinetic constants. The simulation program uses a block simulation approach scheme.	The model has to integrate external models for the processing of certain variables and graphs.	DiToro et al. (1983)

^a TM: Transport Model

^b HM: Hybrid Model

1.2.3. Environmental fate

1.2.3.1. Transport and partitioning

In surface water, PAHs can volatilize, photolyze, oxidize, biodegrade, bind to suspended particles or sediments, or accumulate in aquatic organisms (with bioconcentration factors often within the 10-10,000 range). In sediments, PAHs can biodegrade or accumulate in aquatic organisms (Agency for Toxic Substances and Disease Registry, 1995).

Transport and partitioning of PAHs in the environment are determined to a large extent by physicochemical properties such as water solubility, vapor pressure, Henry's law constant, octanol-water partition coefficient (K_{ow}), and organic carbon partition coefficient (K_{oc}) (Agency for Toxic Substances and Disease Registry, 1995). In general, PAHs have low water solubilities (Agency for Toxic Substances and Disease Registry, 1995). Henry's law constant is the partition coefficient that expresses the ratio of the chemical's concentrations in air and water at equilibrium, and is used as an indicator of a chemical's potential to volatilize. K_{oc} indicates the chemical's potential to bind to organic carbon in soil and sediment, whereas K_{ow} is used to estimate the potential for an organic chemical to move from water into lipid, and has been correlated with bioconcentration in aquatic organisms. Some of the transport and partitioning characteristics (e.g., Henry's law constant, K_{oc} values, and K_{ow} , values) of the 16 PAHs are correlated to their molecular weights. As an example, Hattemer et al. (1991) found low solubility, low vapor pressure, and high K_{ow} of benzo[a]pyrene results in largest presence of the contaminant in soil (82%) and sediment (17%), with $\approx 1\%$ partitioning into the water and $<1\%$ into the air, suspended sediment and biota.

PAHs are present in the atmosphere in the gaseous phase or sorbed to particulates. In general, PAHs having two to three rings (as Naphthalene) are present in the air predominantly in the vapor phase. PAHs with four rings exist both in the vapor and particulate phase, and PAHs having five or more rings (as benzo[a]pyrene) are found predominantly in the particle phase (Baek et al., 1991).

1.2.3.2. Water

PAH compounds tend to be removed from the water column by volatilization to the atmosphere, by binding to suspended particles or sediments, or by accumulation or sorption into aquatic biota (Agency for Toxic Substances and Disease Registry, 1995). The transport of PAHs from water to the atmosphere via volatilization will depend on Henry's law constants for these compounds. The low molecular weight PAHs, such as Naphthalene, have Henry's law constant in the range 10^{-3} - 10^{-5} [atm-m³/mol], while high molecular weight PAHs, such as Benzo[a]pyrene, have values in the range 10^{-5} - 10^{-8} [atm-m³/mol]. Compounds with values ranging from 10^{-3} - 10^{-5} tend to volatilize, while compounds with values less than 10^{-5} volatilize from water only to a limited extent (Agency for Toxic Substances and Disease Registry, 1995). Southworth et al. (1978) stated that lower molecular weight PAHs could be substantially removed by volatilization if suitable conditions (high temperature, low depth, high wind) were present. Even for PAHs susceptible to volatilization, other processes, such as adsorption, photolysis or biodegradation may become more important than volatilization in slow-moving, deep waters (Agency for Toxic Substances and Disease Registry, 1995).

Naphthalene can be removed from water by volatilization, sorption, photolysis, and biodegradation. The relative contributions of these processes will partly depend on the stream's characteristics, including depth, flow rate, and contamination level (Cerniglia, 1992).

1.2.3.3. Sediment

Because of their low solubility and high affinity for organic carbon, PAHs in aquatic systems are primarily found sorbed to settleable particles, or suspended in the water column. There is evidence that two-thirds of PAHs in aquatic systems are associated with particles, and only about one-third is present in dissolved form (Eisler, 1987).

Low molecular weight PAHs have K_{oc} values in the range 10^3 - 10^4 , indicating a moderate potential to be adsorbed to organic carbon in the soil and sediments. On the other hand, high molecular weight PAHs (as B[a]P) have K_{oc} values in the range of 10^5 to 10^6 , indicating stronger tendencies to adsorb to organic carbon (Southworth et al., 1978). Moreover, sorption of PAHs to sediments increases with increasing organic carbon content and with increasing surface area of the sorbent particles (Agency for Toxic Substances and Disease Registry, 1995). In the case of Naphthalene, soil and sediment bind this chemical to a moderate extent depending on soil type. Naphthalene will move rapidly through sandy soil. However, increasing organic carbon content will increase naphthalene's sorption to soil (Cerniglia, 1992).

1.2.4. WWTPs role in PAHs contribution to rivers

Following their release from fuel spillage or atmospheric deposition, PAHs can enter the sewage system through domestic wastewater, industrial discharge, or - mostly - via surface runoff (Liu et al., 2017). Many authors have highlighted the importance of PAHs contamination in urban wastewater. Qiao et al. (2014) reported that WWTP effluent accounted for 60 to 90% of the total PAHs input to the receiving rivers within the Haihe River System. Similarly, Qi et al. (2013) estimated that 80% of the riverine PAHs in the greater Beijing area may be traced to sewer facilities, while Zheng et al. (2016) showed that the riverine PAHs levels closely follow those of the upstream WWTP effluents in the Three Gorges Reservoir region in China. This suggests that WWTPs can be critical points of PAHs discharge to water bodies, with the potential to affect the environment at a local or regional scales.

Tables 1.5 and 1.6 show a summary of various studies that have measured concentrations of Naphthalene and Benzo[a]pyrene, respectively, in municipal treatment plant effluents across the world. WWTPs included in the tables have conventional activated sludge processes (CASP), as the main treatment.

Table 1.5: Concentration of naphthalene in effluents from different treatment plants around the world.

Author	Location	Sampling date	PAH concentration in the effluent (ng/L)	Nº of Samples
Bussetti et al. (2006)	Fusina WWTP, Venice (Italy)	Oct. 2002	26 ± 2	3
Vogelsang et al. (2006)	WWTP A in Oslo (Norway)	Spring and autumn 2002	52.5 ± 19.1	2
Vogelsang et al. (2006)	WWTP B in Oslo (Norway)	Spring and autumn 2003	445 ± 176.8	2
Vogelsang et al. (2006)	WWTO C in Bergen (Norway)	Spring and autumn 2004	105 ± 7.1	2
Vogelsang et al. (2006)	WWTP D in Arendal (Norway)	Spring and autumn 2005	169.5 ± 101.8	4
Vogelsang et al. (2006)	WWTP E in Tromso (Norway)	Spring and autumn 2006	105 ± 7,1	2
Liu et al. (2017)	Guangzhou, China	Nov. and Dec. 2015	80.15 ± 35.72	4
Qiao et al. (2014a)	Beijing (China)	Feb. to Mar. 2013	117 ± 13,3	3
Tian et al. (2012)	Tai'an WWTP (China)	May. 2008	56.7 ± 2	15
Tian et al. (2012)	Tai'an WWTP (China)	Nov. 2008	207.9 ± 18	15
Nas et al. (2020)	Konya WWTP (Turkey)	Sept. 2017 to Aug. of 2018	194 ± 560	16
Pham and Proulx (1998)	Montreal, Canada	Jul. to Oct. 1993	88 ± 49	6
Sun et al. (2018)	Harbin WWTP, Northeast China	2009	74.5 ± 36.6	62 (samples between 2009 and 2016)
Sun et al. (2018)	Harbin WWTP, Northeast China	2010	67 ± 18	
Sun et al. (2018)	Harbin WWTP, Northeast China	2011	119 ± 116	
Sun et al. (2018)	Harbin WWTP, Northeast China	2012	622 ± 388	
Sun et al. (2018)	Harbin WWTP, Northeast China	2014	190 ± 143	
Sun et al. (2018)	Harbin WWTP, Northeast China	2015	898 ± 356	
Sun et al. (2018)	Harbin WWTP, Northeast China	2016	471 ± 261	
Wang et al. (2013)	Hefei, China	Aug. 2011 (wet season) and Dec. 2011 (dry season)	924.4 ± 64.6	
Sánchez-Ávila et al. (2009)	WWTP of Matar in Catalonia, Spain	2007	3490 ± 1800	6
Włodarczyk-Makula et al. (2005)	Poland, Europe	Summer 2003	119 ± 43	N/I
Włodarczyk-Makula et al. (2005)	Poland, Europe	Winter 2003	1045 ± 190	N/I
Man et al. (2017)	Stonecutters Island WWTP in Hong Kong, China	Nov. 2011 to Feb. 2012	34.8 ± 39.9	5
Man et al. (2017)	Shatin WWTP in Hong Kong, China	Nov. 2011 to Feb. 2012	8.75 ± 10.75	5

Table 1.6: Concentration of Benzo[a]pyrene in effluents from different treatment plants around the world.

Author	Location	Sampling date	PAH concentration in the effluent (ng/L)	N° of Samples
Manoli and Samara (1999)	Thessalonik (Greece)	Sept. 1994 to Dec. 1995	4.8 ± 2.7	20
Bussetti et al. (2006)	Fusina WWTP, Venice (Italy)	Oct. 2002	66 ± 3	3
Qiao et al. (2014a)	Beijing (China)	Feb. to Mar. 2013	4.02 ± 0.14	3
Nas et al. (2020)	Konya WWTP (Turkey)	Sept. 2017 to Aug. of 2018	46 ± 70	16
Pham and Proulx (1997)	Montreal, Canada	Jul. to Oct.1993	1 ± 2	6
Sun et al. (2018)	Harbin WWTP, Northeast China	2011	0.8 ± 0.4	62 (samples between 2009 and 2016)
Sun et al. (2018)	Harbin WWTP, Northeast China	2012	10.5 ± 10.5	
Sun et al. (2018)	Harbin WWTP, Northeast China	2014	42.5 ± 29.8	
Wlodarczyk-Makula et al. (2005)	Poland, Europe	Summer 2003	66.48 ± 45.76	N/I
Wlodarczyk-Makula et al. (2005)	Poland, Europe	Winter 2003	5.08 ± 1.69	N/I
Man et al. (2017)	Stonecutters Island WWTP in Hong Kong, China	Nov. 2011 to Feb. 2012	0.21 ± 0.09	5
Man et al. (2017)	Shatin WWTP in Hong Kong, China	Nov. 2011 to Feb. 2012	0.04 ± 0	5

1.2.5. Global regulation of PAHs in aquatic systems

The standards for PAHs concentration limits in drinking water are variable across the world. In the case of the European Union, Council Directive 2008/105/EC on the quality of water intended for human consumption established a maximum limit for benzo[a]pyrene of $0.01 \mu\text{g/L}$, and a maximum of $0.10 \mu\text{g/L}$ for the sum of benzo[b]fluoranthene, benzo[k]fluoranthene, benzo[ghi]perylene and indeno[1,2,3-cd]pyrene. The U.S. federal government established regulatory standards and guidelines to protect people from potential health effects caused by eating, drinking, or breathing PAHs. Under the Safe Drinking Water Act, the US-EPA sets legal maximum limits on the level of Benzo[a]pyrene in drinking water at $0.2 \mu\text{g/L}$ (US-EPA, 2020). In Latin America, only two countries have regulation for PAHs in water, specifically for Benzo[a]pyrene: one is Brazil, with a maximum limit of $0.7 \mu\text{g/L}$ concentration in drinking water (Brazilian Ministry of Health, 2004), and the second is Argentina, with a maximum of $0.04 \mu\text{g/L}$ in water sources for human consumption (Undersecretary of Water Resources of Argentina, 2003).

In the case of Naphthalene, only the US-EPA has defined maximum concentrations in surface runoff and groundwater at a Health Reference Level (HRL) of $140 \mu\text{g/L}$. Further, the agency states that naphthalene is infrequently detected in public water supplies; when detected, naphthalene very rarely exceeds the HRL or a value of one-half of the HRL (U.S. Environmental Protection Agency, 2003).

For sediments, two maximum permissible concentrations (MPCs) were investigated. One is proposed by Kalf et al. and sets the limit to 2,700 [$\mu\text{g}/\text{kg}$]. The second MPC is proposed by Verbruggen in 2012 for the National Institute for Public Health and the Environment of the Netherlands which sets the limit at 490 [$\mu\text{g}/\text{kg}$], the most stringent limit reported among the reviewed regulations.

In Chile, PAHs are not included in the current regulation. For example, the DS 90/2000 regulates the discharge of treated effluent to marine and continental surface waters, does not include organic contaminants of kind. Other related regulations such as the NCh1333, which sets water quality requirements for different uses (including irrigation), only consider basic parameters for soil maintenance. Regarding reuse applications, the Ley 21.075/2018 regulates the collection and disposition of grey water urban and rural areas, does not include emerging or persistent pollutants.

1.2.6. WWTP effluent reuse on agricultural irrigation

Effluents from sewage plants are emerging as a major source of direct discharge of PAHs into water bodies in urban areas. Treated water is used for crop irrigation and, in some cases, treated downstream again for potable use. *De facto* reuse occurs when water intakes draw raw water supplies downstream of clean water discharges from sewage or wastewater treatment plants (WateReuse Association, 2017). This is observed in the Maipo River basin, where reuse is mainly for irrigation. Water quality standards of reclaimed water irrigation (RWI) in developed countries have been established to ensure safe irrigation (Bastian & Murray, 2012). These guidelines have prescribed acceptable concentrations of bulk parameters such as Chemical Oxygen Demand (COD), Biochemical Oxygen Demand (BOD), and heavy metals. However, organic pollutants like PAHs are not specifically regulated.

On the other hand, the literature provides certain guidelines as to what are the consequences of reusing water for agricultural purposes from water containing PAHs. Haddaoui et al. (2016) reported concentrations of PAHs in soils irrigated with wastewater in Nabeul, Tunisia. They analyzed 13 types of PAHs in soil samples collected from surface strata at 0-10 and 10-20 cm depth, before all irrigations performed in the area and after the irrigation period, extending from June to October. From this, it was obtained that the total concentration of PAHs varied between 120.01 and 365.18 $\mu\text{g}/\text{kg}$ dry weight, at 0-10 cm depth, before and at the end of irrigation, respectively. Further, it could be noted that 4-ring PAHs were the predominant group in terms of presence, both in the upper soil layer and in the lower layer. Haddaoui et al. (2016) concluded that agricultural practices, including irrigation, are the origin of the progressive increase of PAHs concentrations in the soil.

Zhang et al. (2017) studied soils irrigated with farmland wastewater in Tongliao City, located in eastern Inner Mongolia and one of the most important industrial and agricultural cities in China. The water used for irrigation comes from the West Liao River, which flows through the city and receives effluent from both treated/untreated industrial wastewater and local municipal wastewater. Through the examination of uptake from 16 priority PAHs and five heavy metals from soils intended for corn cultivation with wastewater irrigation, this study revealed the effects of heavy metals on PAHs uptake in terms of co-contamination. The results from 15 investigated soils showed a medium level of contamination, and the

vertical distribution of PAHs in soils indicated that 2-3-ring PAHs were easier to transport in soils, causing a great potential risk of immigrating to groundwater. Three-ring PAHs were more likely to be taken up by corn roots, while two- and four- to six-ring PAHs were less likely. Additionally, the translocation of PAHs in corn tissues was found to have a positive relationship with the logarithm of the octanol-water partition coefficient ($\log K_{ow}$) below 4.5, while for a value above 4.5, it has a negative correlation. This, according to the authors, posed health risks due to the potential for accumulation in corn grains.

Azouzi et al. (2016) examined the effects of long-term irrigation with treated wastewater in three soil types (lithosol, saline soil, and isohumic soils) as a function of PAHs content in Draa Tammar, located in the central region of Tunisia (semi-arid climate). The perimeter irrigated by Draa Tammar, with treated sewage, showed elevated PAHs concentrations. The mean concentration of total dry matter PAHs was 2252.18 $\mu\text{g}/\text{kg}$ for the three soils; ranging from 204.16 $\mu\text{g}/\text{kg}$ (at 20-40 cm level of isohumic control soil) to 8845.41 $\mu\text{g}/\text{kg}$ (at 20-40 cm level of lithosol). In general, the highest amounts of total PAHs were always found in the most superficial strata of soils (0-20 cm layers). In this study, irrigated soils were found to be highly contaminated, and concentrations of carcinogenic molecules were about 1.2 to 7.6 times higher (depending on the soil type evaluated) in these perimeters than in control soils. In summary, the results of the study showed that soil texture and mineralogy, water quality and volume, soil fauna, and root respiration are key parameters controlling the retention of PAHs in the soil.

1.3. Objectives

The general objective of this work is to study and model the fate and effect of two Polycyclic Aromatic Hydrocarbons (PAHs), Naphthalene and Benzo[a]pyrene, in the downstream section of the La Farfana WWTP discharge point into the Mapocho River (Santiago, Chile).

The specific objectives of this work are:

- Study the fate and distribution of PAHs in the Mapocho River using the WASP-8 model and HEC-RAS coupled model.
- Analyze the influence of relevant parameters (i.e., streamflow and PAHs loading) on the estimation of PAHs concentrations in the river.
- Determine possible consequences for water reuse in the Metropolitan Region.

Chapter 2

Methodology

2.1. Study area

2.1.1. Mapocho river in Santaigo, Chile

The Mapocho River basin covers a large part of the city of Santiago (capital of Chile), draining an area of 4015 km². The main river has a length of 110 km, with headwaters in the El Plomo Mountain (~5000 m.a.s.l. in the Andes Cordillera), flowing in a northeast-southwest direction through sixteen municipalities across the city of Santiago. The basin has a mixed hydrologic regime, dominated by snowmelt in spring and summer, with streamflow increments during winter due to rainfall events. Further, the Mapocho River provides water for irrigation of 10,000 ha agricultural areas. The main characteristics of this basin are shown in Table 2.1.

Table 2.1: Catchment attributes. Source: Alvarez-Garreton et al. (2018).

Catchment Attributes	
Name ^a	Río Mapocho en Rinconada de Maipú
ID ^a	5737002
Catchment Outlet [lat, long]	-33.4961 S, -70.8167 E
Area [km ²]	4014,7
Catchment Outlet elev. [m.a.s.l.]	432
Catchment mean elev. [m.a.s.l.]	1343
Catchment max. elev. [m.a.s.l.]	5431
Mean slope [m/km]	155,9
Annual Precip. (CR2MET) [mm]	408
Human intervention degree	3,451

^a CAMELS-CL CR2MET Atributtes

The Mapocho river crosses the city of Santiago (with 7,5M inhabitants, is the most populated city in Chile) and receives effluents from 6 WWTPs in the region. Figure 2.1 shows the study area (red box) including the location of WWTPs and hydro-meteorological stations used to provide data for this study. In this study, only the discharge from the La Farfana plant is considered.

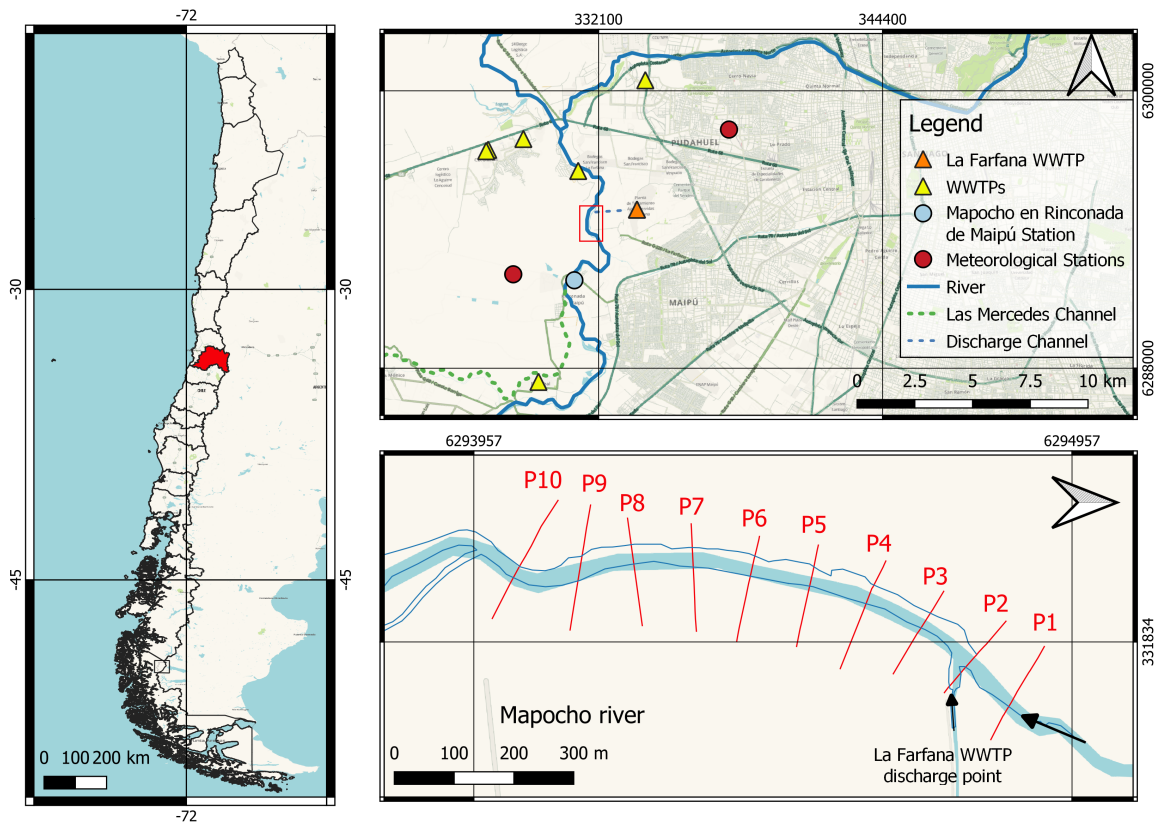


Figure 2.1: Study zone (red box in top right panel) including near WWTP, channels, stations, and river profiles. Map of Chile is in the geographic coordinate system. Map of Santiago and the river profiles are in UTM zone 19S coordinates.

2.1.2. Hydrometeorological and Water Quality Data

2.1.2.1. Data sources

The hydrometeorological input variables used in this study are river flow, air and water temperature, direct solar radiation and wind speed. Additionally, total suspended solids (TSS) are of interest for water quality assessments. Table 2.2 summarizes the different sources and types of information used to characterize the study zone.

Table 2.2: Source and type of input data.

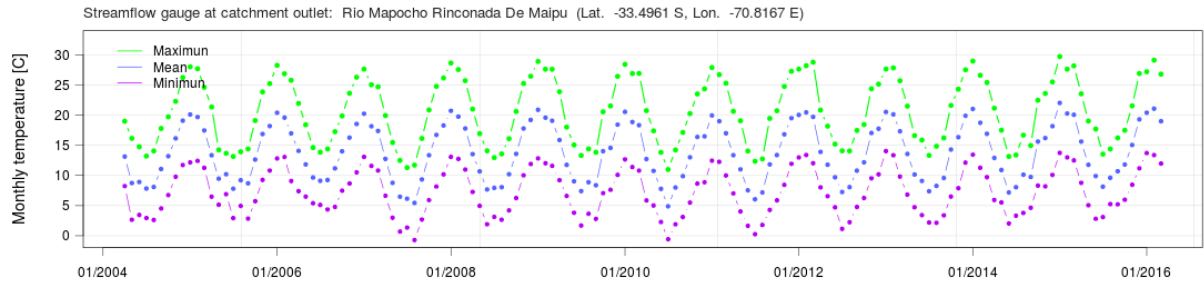
Source	Type	Data
CAMELS-CL (CR2 ^a)	Data base	Streamflow, Air temperature
Solar explorer	Gridded product	Wind speed, Solar radiation
Aguas Andinas	On-site measurements	Total suspended solids (TSS)
DGA ^b	On-line Station	Water temperature

^a Center for Climate and Resilience Research. <https://camels.cr2.cl/>

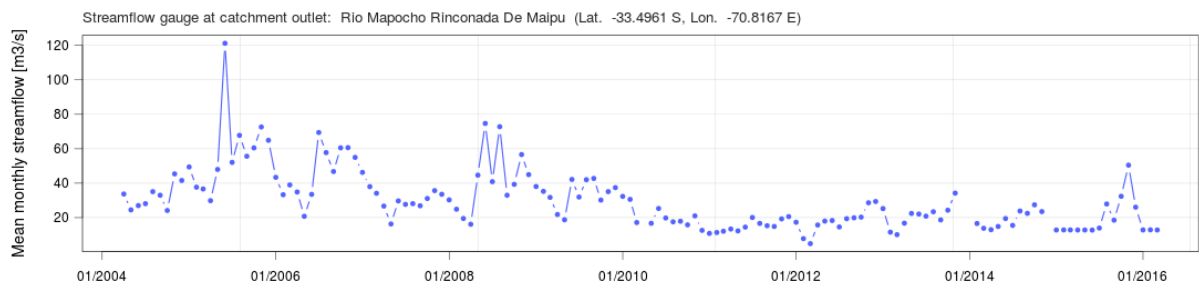
^b Dirección General de Aguas de Chile. <https://snia.mop.gob.cl/BNAConsultas/reportes>

2.1.2.2. Mapocho's hydrometeorological data

Streamflow data and air temperature data were obtained from the CAMELS-CL dataset, based on real-time records of DGA on-line fluviometric station (Alvarez-Garreton et al., 2018). Figure 2.2 shows the temperature and streamflow records obtained from the Mapocho station at Rinconada de Maipú. The monthly data series corresponds to the period April/2004 – March/2016.



a Maximum, mean, and minimum monthly temperature.



b Mean monthly streamflow.

Figure 2.2: Streamflow and temperature records for the Rinconada de Maipú station from April/2004 to March/2016..

Figure 2.3 displays 41 water temperature data from May 2004 to March 2016 that were obtained from the Rinconada de Maipú station (DGA, Chile).

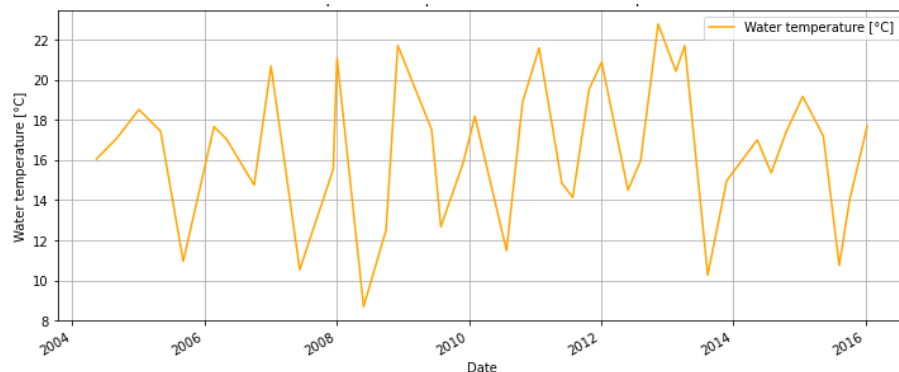


Figure 2.3: Water temperature data from the Rinconada de Maipú station from April/2004 to March/2016.

On the other hand, hourly information of direct solar radiation (in W/m^2) and wind speed (in m/s) is obtained from the gridded product of the Solar Explorer for the studied

period. Both data (wind speed and solar radiation) are entered at an hourly level from April 2004 to March 2016. An example of input time functions for solar radiation and wind speed is presented in Appendix B.2.

2.1.2.3. Total Suspended Solids

Monthly data of the total suspended solids (TSS) in the water column were obtained from the local sanitation company (Aguas Andinas S.A. – Private communication). Figure 2.4 shows the river's TSS concentration downstream WWTP from April 2004 to December 2012.

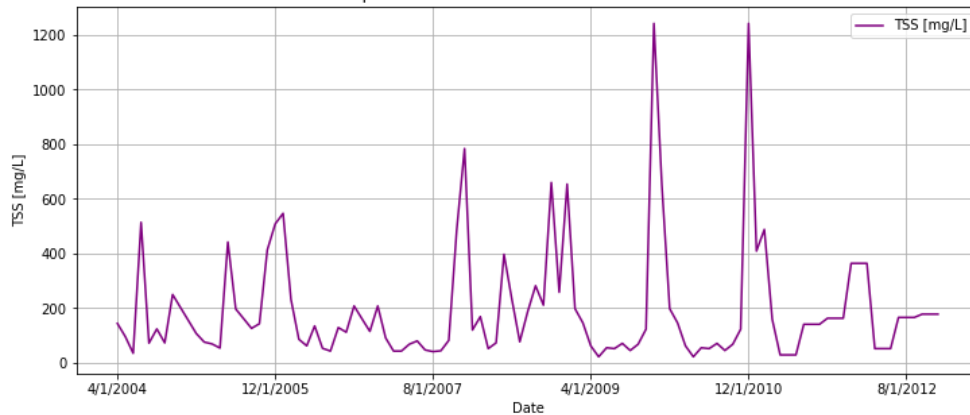


Figure 2.4: Total Suspended Solids data measured by Aguas Andinas from April/2004 to December/2012.

2.1.3. La Farfana WWTP

La Farfana is the largest WWTP in Chile and one of the two largest treatment plants in Santiago. It started operating in October 2003 and it serves a population of 3,294,000 PE. La Farfana uses conventional activated sludge for water treatment and anaerobic digestion for sludge stabilization. The average design treatment flow is 8.8 m³/s per day (760,320 m³/d), and its maximum capacity is 15 m³/s for the maximum hourly flow (Dirección General de Aguas de Chile, 2004). Figure 2.5 shows a time series with average monthly effluent flows for the period April/2004 - March/2016, which have been increasing since the installation of the plant.

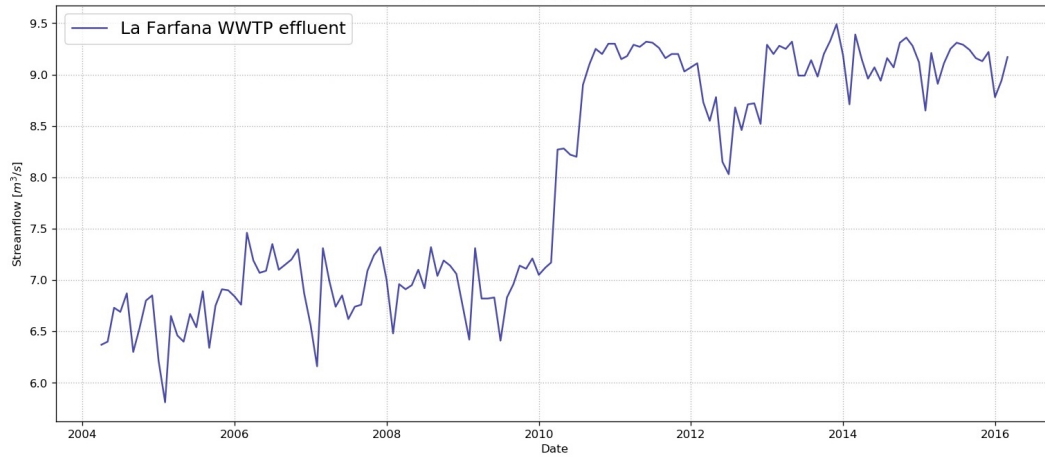


Figure 2.5: Evolution of La Farfana WWTP effluent from April 2004 to March 2016. Data provided by Aguas Andinas S.A.

2.1.4. River characterization

The hydraulics of the study area is analyzed with information provided by the National Hydraulic Institute of Chile (INH, for its acronym in Spanish), which includes bathymetry (i.e., river’s cross-sectional profiles) along one kilometer downstream the effluent discharge point, general descriptions of the area, and soil test pits on the riverside (INH, 2016). Based on the previous information, silts and fine grained soils were predominant in the study area. The cross-sectional profiles and location of the discharge point are shown in Figure 2.1.

2.2. Conceptual model development

In this study, we adopt a modeling framework that combines the HEC-RAS model (Brunner, 2016) – which represents hydraulic processes –, and the WASP8 Model (R. B. Ambrose & Wool, 2017), which brings together the chemical, hydrological and hydraulic variables under consideration. The US-EPA WASP8 model is selected for water quality because of its user-friendly interface and the constant improvements and updates by its developer. Figure 2.6 shows a conceptual scheme of the models and variables that are coupled for the work. It shows the transport and transformation processes that take place in rivers, and the interaction between the different phases in the water column. It should be noted that the outputs from HEC-RAS (e.g., mean depths and widths, river cross-sectional areas, and segment volumes) serve as inputs for the WASP8 model.

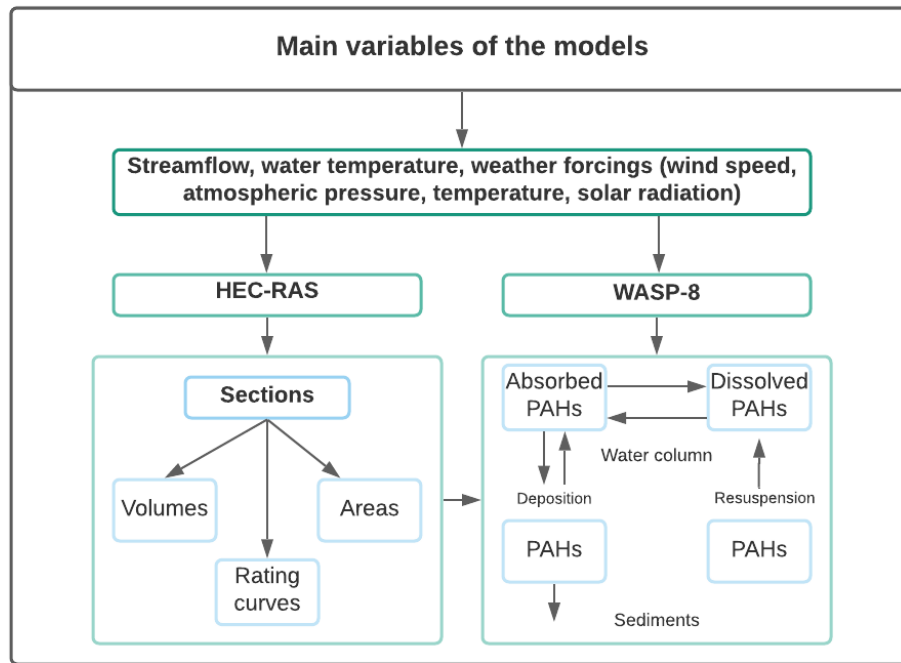


Figure 2.6: Conceptual model of PAHs fate and transport. Modified from Jaco (2020).

2.2.1. HEC-RAS Model

In this study, HEC-RAS is used for hydrodynamic modeling of the case study river section. Simulations were performed for the average monthly flows from April 2004 to March 2016 to obtain velocity, runoff depth, area, volume, and top width of the river sections. These were used to define the geometry into the WASP8 model and to calculate the dispersion coefficient for each segment. Steady flow simulations were conducted with normal head boundary conditions for both upstream and downstream of the river reach, considering a mixed flow regime. A Manning’s roughness coefficient of 0.035, corresponding to sand sediments, was used for the main channel, and a Manning’s coefficient of 0.04 for banks with overhanging bushes, as shown in Figure D.1 in Appendix D (Barnes, 1969; Chow, 1959).

2.2.2. WASP8: Water Quality Analysis Simulation Program

The Water Quality Analysis Simulation Program (R. B. Ambrose & Wool, 2017) is a generalized framework for modeling contaminant fate and transport in surface waters, facilitating decision-making in water management problems. The model does not solve a set of multi-dimensional dynamical equations; instead, it is based on a flexible compartment modeling approach. WASP8 can be applied in one, two, or three dimensions, and time-varying advection, dispersion, point and diffuse mass loading, and mass exchange are represented in the model. WASP8 has been applied for several applications, including biochemical oxygen demand and dissolved oxygen dynamics, nutrients and eutrophication, bacterial contamination, and organic chemical and heavy metal contamination.

A water body is represented in WASP8 as a series of computational elements or segments. Environmental properties and chemical concentrations are assumed to be spatially constant within segments. Segment volumes and type (surface water, subsurface water, surface benthic, subsurface benthic) must be specified, along with hydraulic coefficients for riverine networks.

It is important to note that the interaction between hydrodynamic, chemical, and hydrological processes involves internal processes that are more complex and difficult to model. The simplification of these interactions through the use of models such as WASP8 provides a better understanding of the reality and a notion of which processes the pollutant goes through when it enters the water body. Transformation and degradation processes such as sorption, volatilization, photolysis, oxidation, biodegradation, and hydrolysis are included in the model. WASP8 also includes both water column and sediment segmentation and descriptive transport (e.g., resuspension, sedimentation, burial) for the sediments and associated contaminants between the bed and water column, as illustrated in Figure 2.7. Additionally, chemical partition (to dissolved organic carbon and solids) and reaction (phototransformation, biodegradation) processes are modeled in the framework.

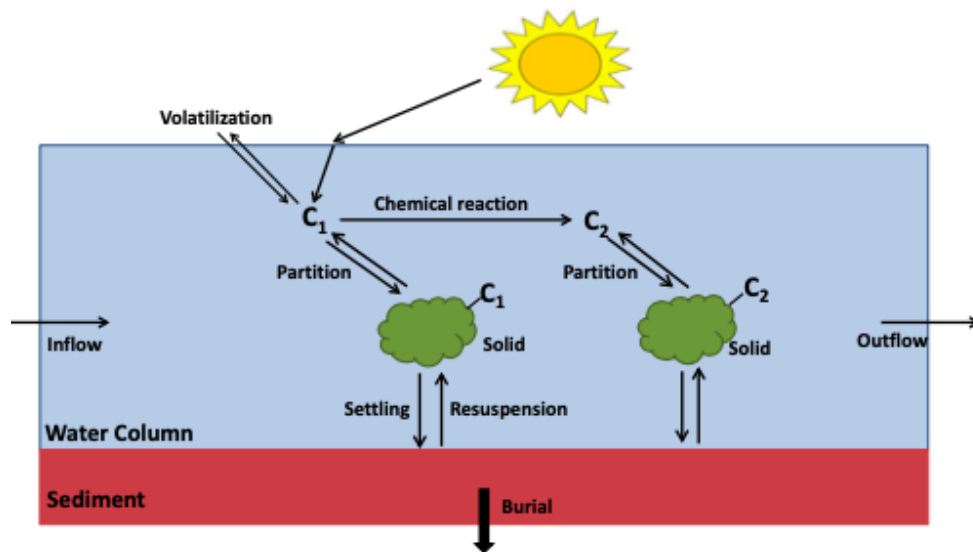


Figure 2.7: Framework and processes for the Advanced Toxicant module. Source: Wool et al. (2020)

2.2.2.1. Hydrometry

For the hydrodynamic linkage flow option, velocities and depths computed by the hydrodynamic model are used in WASP. For the internal flow options (Net Flow, Gross Flow, Kinematic Wave), a set of user-specified hydraulic discharge coefficients defines the relationship between velocity, depth, and streamflow in surface water segments.

2.2.2.2. Governing Flow Equations

The WASP streamflow model consists of a set of one-dimensional equations solving water flow and water volume in a branching stream or shallow river network. This network can

include free-flowing stream reaches (kinematic wave flow), ponded reaches (weir overflow), and backwater or tidally influenced reaches (dynamic flow). The equation of motion, based on the conservation of momentum, predicts water velocities and flows. The equation of continuity, based on the conservation of volume, predicts water heights (heads) and volumes. The equations in the model are described in detail in Appendix A.2. Kinematic wave flow was the selected stream reach for solving water flow, and the associated equations are included in Appendix A.3.

2.2.2.3. WASP Transport Fields

Advective transport in WASP is divided into six distinct types, or "fields" (see Appendix A.4 for detail). In this case, the first transport field is used, which involves advective flow and dispersive mixing in the water column. The advective flow transports water quality components "downstream" with the water, and dilution is also considered. Dispersion causes further mixing and dilution between regions of high concentrations and regions of low concentrations.

For each type of transport, dispersion coefficients (in m^2/s) as a function of time need to be provided, and they vary along each river section. For each interchange between segments, an interfacial area, mixing length, and the contiguous segments between which the interchange takes place should be provided. The characteristic mixing length is specifically the distance between the midpoints of each segment. The interfacial area is the area normal to the characteristic mixing length shared with the simulated segments (cross-sectional area for horizontal exchanges or surface area for vertical exchanges). The longitudinal dispersive transport of a conservative substance is modeled in WASP by a one-dimensional advection-dispersion equation (see Appendix A.5). The advection-dispersion equation requires specifying dispersion coefficients (see section 2.4 for details).

2.2.3. Model considerations

Some considerations and assumptions of the modeling framework adopted in this study are listed below:

1. Simulations are performed in steady state with monthly temperature and streamflow data, and with hourly wind speed and solar radiation data. The simulation period starts on April 1, 2004 and ends on March 31, 2016.
2. Although streamflow data was obtained from the Mapocho en Riconada de Maipu Station from CAMELS-CL dataset (Alvarez-Garreton et al., 2018), the maximum river flow before flooding was set at $50 \text{ m}^3/\text{s}$.
3. For the studied river section, PAHs contributions by tributaries or diffuse sources are not considered.
4. The following state variables are selected for simulation: two organic chemicals, Benzo[a]-pyrene and Naphthalene, and one solid, named TSS (for Total Suspended Solids). For the river segments definition, kinematic wave stream flow option was implemented. Only surface water segment types were included, as subsurface water and benthic segments need to be included only if sediment transport is considered.

5. To simplify the analysis in WASP8, the density and diameter of the TSS particles were set as those of silt and sediment transport was neglected. Transfer processes defined in the model include sorption and volatilization. These are described by first-order rate equations. Sorption is modeled as an equilibrium reaction. The selected numerical solving technique in the water quality module is the Euler solution.
6. WWTP’s effluent concentrations were considered constant throughout the entire study period (2004 to 2016). The methodology followed to obtain the PAHs concentrations by percentiles is presented in Section 2.3.
7. Due to the lack of information on TOC (Total Organic Carbon) in the water and sediment phases, these values were obtained from the literature based on the river’s sediment characteristics (i.e., sandy-silty sediments). TOC content is fundamental to define K_{ow} and K_{oc} partitioning coefficients (see section 1.2.3.1).
8. The chemical properties constants entered into the model are shown in Table 2.3. The data presented have been extensively used and obtained from the National Center for Biotechnology Information (2021).

Table 2.3: Benzo[a]pyrene and Naphthalene Chemical properties.

Benzo[a]pyrene Chemical Properties (at 25°C)			
Molar mass [g/mol]	252.3	Vapor pressure [Pa]	negligible
Density [g/cm ³]	1.24	Water solubility [mg/L]	$1.62 \cdot 10^{-3}$
Half-life degradation [days]		Log octanol-water partition coefficient [log Kow]	6,13
in Water	12 to 23	Organic carbon partition coefficient [Koc]	$2.7 \cdot 10^5$ to $1.9 \cdot 10^6$
in Sediment	229 to 309	Henry’s Law constant [atm/mole/m ³]	$4.57 \cdot 10^{-7}$
Naphthalene Chemical Properties (at 25°C)			
Molar mass [g/mol]	128.17	Vapor pressure [Pa]	11
Density [g/cm ³]	1.14	Water solubility [mg/L]	31
Half-life degradation [days]		Log octanol-water partition coefficient [log Kow]	3.3
in Water	0.8 to 43	Organic carbon partition coefficient [Koc]	112 to 9333
in Sediment	1.1	Henry’s Law constant [atm/mole/m ³]	$4.40 \cdot 10^{-4}$

9. Solids transport constants entered into the model are shown in Table 2.4. These values correspond to a silty type as suspended sediment.

Table 2.4: Selected constants for the Solids transport module in WASP simulation.

Constant	Value	Reference	Observation
Sediment temperature [C°]	25	Ambrose et al. (2017)	Assumed value. Default value of WASP.
Particle diameter for solid [mm]	0.025	Ambrose et al. (2017)	Characteristic value of silt
Organic carbon fraction [-]	0.016	Chiou et al. (1998)	From Mississippi river sediment sample (USGS sample campaigns)

10. Chemical partitioning and kinetic sorption constants entered into the model correspond to values obtained from literature, as shown in Table 2.5. These values correspond to data adjusted to sandy-silty sediments.

Table 2.5: Selected constants for the Chemical partitioning and Chemical Kinetic sorption modules in WASP simulation.

Module	Constant	Value	Reference	Observation
Chemical Partitioning	Partition coeff. of Nap to DOC [L/kg]	215	Burkhard (2000)	Report relating the values of this coefficient to the octanol-water coefficients of the pollutants.
	Partition coeff. of B[a]P to DOC [L/kg]	467735		
	Partition coeff. of Nap to solid [L/kg]	11.4	Chiou et al. (1998)	Obtained from the foc values proposed by the author together with the octanol-water coefficients using the expression $K_d = K_{oc} \cdot f_{oc}$
	Partition coeff. of B[a]P to solid [L/kg]	1077.6		
Chemical Kinetic Sorption	Sorption rate to solid [L/kg-day] for Naphthalene	0.0004	Shi et al. (2020)	Obtained from the sorption coefficient calculated by the authors for silt sediments
	Sorption rate to solid [L/kg-day] for B[a]P	0.5	Bowman et al. (2002)	Obtained from the sorption coefficient calculated by the authors for silt sediments

11. To include the volatilization effects of these chemicals, time series of atmospheric concentration of Naphthalene and Benzo[a]pyrene are obtained from Sierra et al. (2005), for the Providencia area, Santiago. The values included in the model for winter (April to September) and spring (October to March) are shown in Table 2.6. It is important to note that these are reference values, since they only consider the presence of PAHs in particulate matter PM10, which has also increased its concentration since the year in which the measurements were taken (the year 2000). To make a more detailed analysis of PAHs concentrations in the air, the changes in the concentration of PM10 over time should be included, and the PAHs concentrations should be calculated proportionally to this increase. Despite being a representative series only for the year 2000, it will be used as a reference series for the years 2004 to 2016 due to the lack of more updated data.

Table 2.6: Mean, minimum, and maximum PAHs concentrations (ng/m^3) in PM10, at Providencia in 2000. Source: Sierra et al., 2005.

	Winter Concentration (ng/m^3)			Spring Concentration (ng/m^3)		
	Mean	Minimum	Maximum	Mean	Minimum	Maximum
Nap	0.19	0.03	0.33	0.08	0.02	0.12
BaP	5.28	2.58	9.49	0.93	0.32	1.47

2.3. Determination of PAHs concentration in WWTP effluents

In the absence of in situ measurements, it was decided to work with values collected from the available literature. Hence, synthetic concentrations can be defined from these values that can be associated with different probability percentiles.

This approach is based on the construction of artificial data sets from a real dataset, by resampling the values collected. Sometimes these methods are also known as resampling tests, randomization tests, re-randomization tests, or Monte Carlo tests. Resampling methods are highly adaptable to different testing situations, and there is considerable scope for the analyst to creatively design new tests to meet particular needs (Wilks, 2011). In this work, a *bootstrap* or resampling was performed. This process is repeated a large number, $n_B = 100,000$ times, yielding n_B bootstrap samples, each of size $m = 8$.

Different concentrations of Naphthalene and Benzo[a]pyrene for different WWTPs in the world were collected from previous studies (See Table 1.5 and Table 1.6). Two main criteria were followed for selecting these plants: 1) the water treated by the plant must have a minimum of 50% of municipal or domestic water, and 2) the plant must conduct similar treatments as those considered in La Farfana WWTP.

With the different concentrations of PAHs in the effluents of various WWTPs around the world, a bootstrap is performed. This non-parametric technique is applied to find the distribution of the mean, by taking random sub-samples of the original sample (25 concentration data for Naph and 11 data for B[a]P), where for each of these sub-samples an average is calculated and the value is stored in an empty list. This generates a histogram of these values, along with the theoretical curve associated with different probability distributions. With the results of the goodness-of-fit tests for each distribution, the parametric distribution that best fits these data is chosen. Together with that distribution, the percentiles associated with the concentration of the compounds studied are determined. For modelling purposes, the concentrations obtained associated with the 10th, 50th and 95th probability percentiles (C_{10} , C_{50} and C_{95}) will be used as input (WWTP effluent concentrations).

2.4. Dispersion coefficient estimates

To estimate the dispersion coefficient in the Mapocho river (D_L), the expression developed by Fischer et al. (1979) was used:

$$D_L = 0.011 \frac{\bar{u}^2 W^2}{du^*} \quad (2.1)$$

Where \bar{u} is the mean velocity in the segment, W is the mean width of the segment, d is the runoff depth and u^* is the shear velocity.

For river base case, the shear velocity can be calculated by Manning's equation:

$$u^* = \langle u \rangle \frac{n}{a} (gR_h^{-1/3})^{0.5} \quad (2.2)$$

Where:

- n is the Gauckler–Manning coefficient [$\text{s}/\text{m}^{1/3}$].
- R_h is the hydraulic radius [m]

Dispersion coefficients of each section of the river section are calculated using each average monthly flow data. An example calculation for each segment is shown in Table B.1.

Chapter 3

Results and Discussion

3.1. River geometry

Table 3.1 summarizes the geometric data obtained from the HEC-RAS model. The slope of the riverbed is $\sim 0.2\%$ and the average segment widths span from 20 to 50 m on its main axis.

Table 3.1: Channel geometric data associated with river cross-sections.

Segment	Profiles	Length between profiles [m]	Average Width [m]	Average Depth [m]	Cross-sectional area [m ²]	Volume [m ³]
1	1 to 2	98.79	49.01	1.49	73.25	7320
2	2 to 3	99.88	50.08	1.80	81.94	8180
3	3 to 4	99.92	22.42	2.03	45.56	4540
4	4 to 5	99.63	22.72	2.18	49.52	4950
5	5 to 6	99.98	26.98	2.16	57.47	5740
6	6 to 7	99.75	28.59	1.91	54.60	5530
7	7 to 8	99.96	30.59	1.92	58.95	6200
8	8 to 9	97.75	41.12	1.88	76.73	8020
9	9 to 10	99.46	38.61	1.91	72.58	7220

3.2. PAHs concentrations in municipal WWTPs effluents

The adjusted theoretical probability density function (PDF) curves for Naphthalene and Benzo(a)pyrene are shown in Figure 3.1 with their respective Q-Q plots. For Naphthalene, the curves show the best fit for the data generated by bootstrap resampling is a log-gamma distribution, and both Chi-squared and Kolmogorov-Smirnov ($> 5\%$) goodness of fit tests were passed. For benzo(a)pyrene, the curves show the best fit for the data is a gamma distribution, and only the Chi-squared was passed and had the minimum square error. This is probably due to the small amount of data used to generate the bootstrap.

Table 3.2 shows the Naphthalene and Benzo(a)pyrene effluent concentrations associated to the percentiles in each distribution. For Naphthalene the values range from 0.06 [$\mu\text{g/L}$] to 0.28 [$\mu\text{g/L}$], and for benzo(a)pyrene, values range from 0.004 [$\mu\text{g/L}$] to 0.035 [$\mu\text{g/L}$].

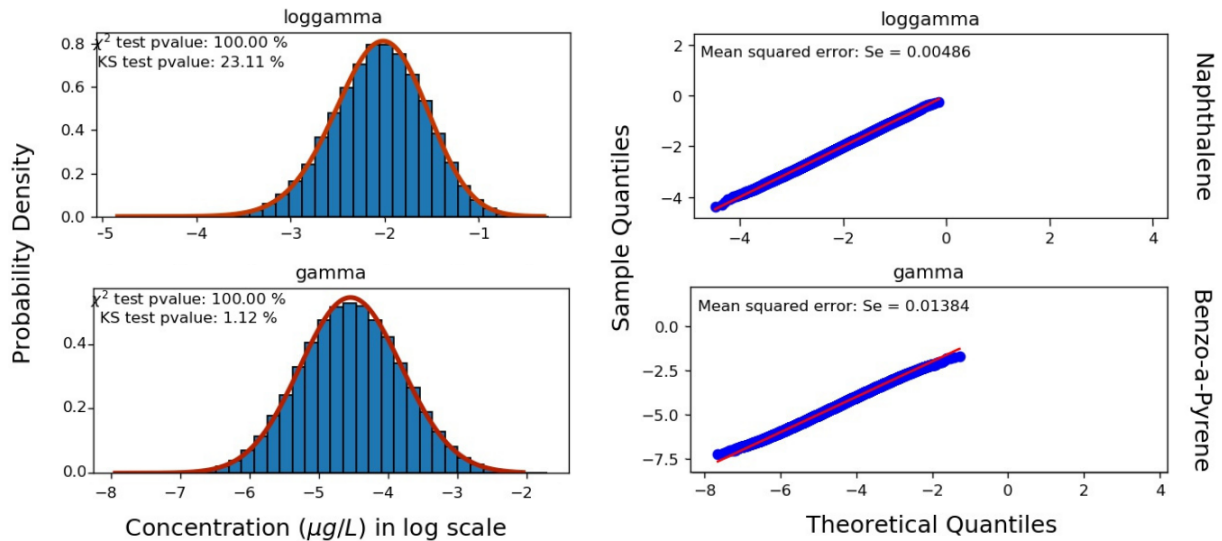


Figure 3.1: Probability distribution function and Q-Q plot for Naphthalene and Benzo[a]pyrene.

Table 3.2: Percentiles of simulated PAHs values.

Concentration according to percentile	Naphthalene [$\mu\text{g}/L$]	Benzo[a]pyrene [$\mu\text{g}/L$]
C_{10}	0.06777	0.00421
C_{20}	0.08531	0.00579
C_{30}	0.10034	0.00729
C_{40}	0.11499	0.00889
C_{50}	0.13035	0.01070
C_{60}	0.14748	0.01289
C_{70}	0.16798	0.01574
C_{80}	0.19512	0.01989
C_{90}	0.23910	0.02755
C_{95}	0.28173	0.03610

Is important to note that the use of a bootstrap relies on having enough data for the underlying population or generating process to have been reasonably well sampled. A small sample, like in this case, may exhibit too little variability for bootstrap samples drawn from it to adequately represent the variability of the generating process that produced the data.

An improvement to the bootstrap process would be to obtain various concentrations of C_{10} , C_{50} and C_{95} using empirical functions to generate a boxplot with minimum, mean (Q2 quartile) and maximum values. By simulating with this range of values, the spectrum of expected concentrations in each case would be better represented. Also, in future opportunities it is suggested not to apply logarithm to the data as was done in this case, in order not to alter the sample significantly.

For modelling purposes, WWTP’s effluent concentrations were considered constant throughout the entire study period (2004 to 2016). This is unrealistic, considering that there is evidence of high seasonal variability of PAHs concentrations in water bodies (see section 1.1.5). However, in the absence of in-situ measurements of PAHs concentrations in the WWTP effluent, this option is considered to be a practical way to simulate within a range of expected concentrations based on literature data.

3.3. Dispersion Coefficient

The dispersion coefficients obtained for each segment are shown in Figure 3.2. These results are considered valid for flows in open channels, with low mixing flow intensity, and under hydraulic conditions similar to the Mapocho River, such as mean velocity, depth, and width of section (Fischer et al., 1979).

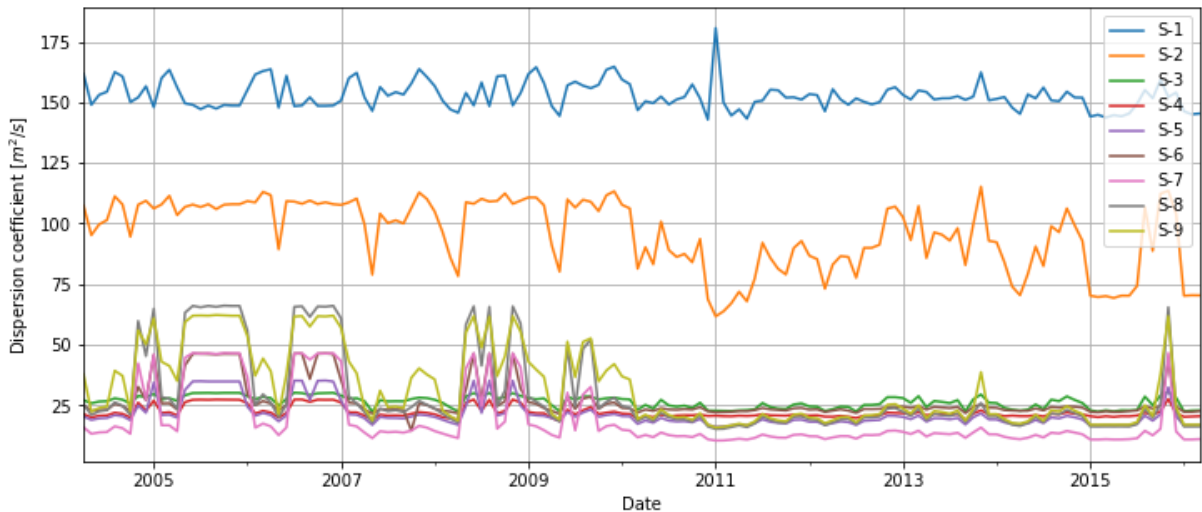


Figure 3.2: Dispersion coefficient series for each river segment from April 2004 to March 2016.

For segments S-3 to S-9, dispersion coefficients (D_L) are within expected values according to Fischer et al. (1979). D_L values are similar for sections S3-S9 due to similarities in their runoff depth (d) and flow velocity (Q) (Eq. 2.1). Also, these sections are downstream of the discharge of the La Farfana, where there are no changes or disturbances in the flow. For S-1 and S-2, higher values of D_L may be due to the boundary conditions upstream of the study segment. Values obtained for Segment S-1 were disregarded from the analysis because they exceeded reported values in literature (Fischer et al., 1979).

3.4. Fate of PAHs in the Mapocho River

WASP8 model simulations are performed using C_{10} , C_{50} and C_{95} , the 10th, 50th and 95th percentiles for Naphthalene ($C_{10} = 0,068 \mu\text{g/L}$, $C_{50} = 0,13 \mu\text{g/L}$ and $C_{95} = 0,282 \mu\text{g/L}$) and Benzo[a]pyrene ($C_{10} = 0,004 \mu\text{g/L}$, $C_{50} = 0,012 \mu\text{g/L}$ and $C_{95} = 0,036 \mu\text{g/L}$) concentrations in the WWTP effluent.

Results from the coupled model are presented in this section. Figure 3.3 shows the evolution of dissolved Naphthalene in segment S-9, approximately 1 km downstream from the discharge point.

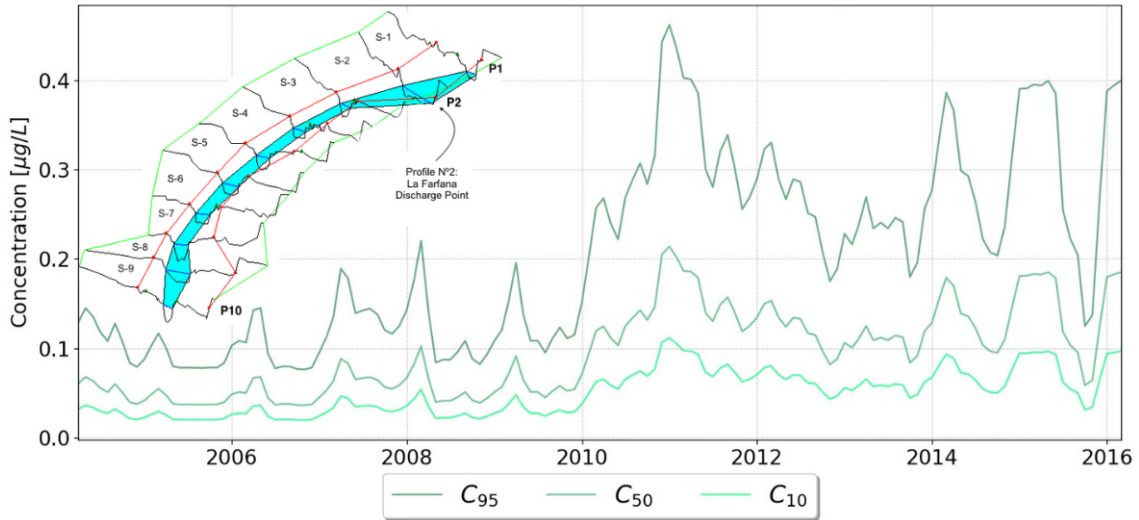


Figure 3.3: Dissolved Naphthalene concentration in river segment S-9 (last segment) for C_{10} , C_{50} and C_{95} .

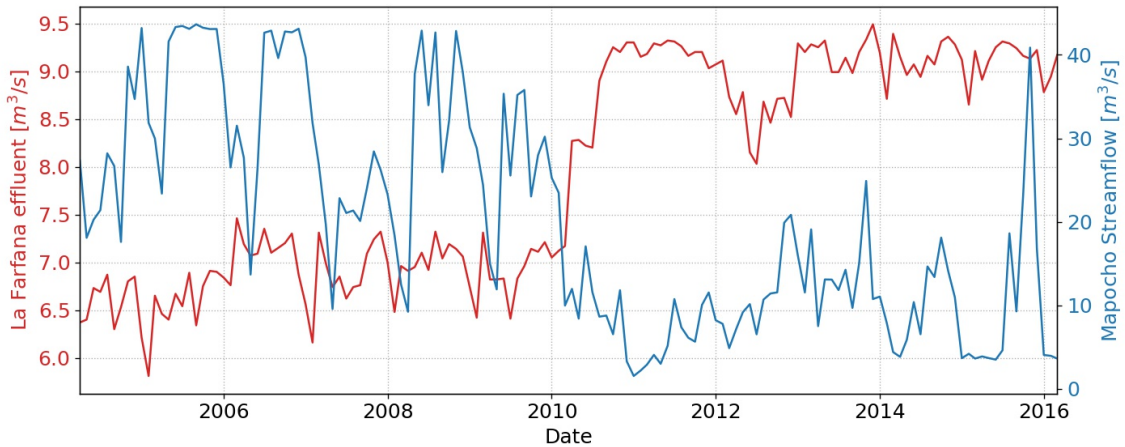


Figure 3.4: La Farfana WWTP effluent and Mapocho streamflow (prior to confluence with discharge point) from April 2004 to March 2016.

The figure shows the increase in Naphthalene concentration due to the incremental discharge flow from the La Farfana plant since 2010 and the progressive decrease in the river's flow since 2009 (see Figure 3.4). Besides, it is observed that the peaks obtained in the series are found in the summer months. The mean dissolved concentrations in segment S-9 for the study period obtained were: $C_{95} = 0,203$ [$\mu\text{g/L}$], $C_{50} = 0,095$ [$\mu\text{g/L}$] and $C_{10} = 0,05$ [$\mu\text{g/L}$]. All the simulated naphthalene values are below the Health Reference Level (HRL) defined by the US-EPA of 140 $\mu\text{g/L}$. These results were expected since Naphthalene is infrequently detected in public water supplies (U.S. Environmental Protection Agency, 2003), and even in the most likely scenario (C_{95}), this might not present a concern for *de facto* reuse. The

sorbed concentrations of Naphthalene were negligible (data not shown), mostly due to its physicochemical characteristics. Naphthalene tends to volatilize for the most part, and to a lesser extent to dissolve.

Figure 3.5 and Figure 3.6 show the distribution of dissolved and sorbed Benzo[a]pyrene to TSS in S-9. Figure 3.5 shows the dissolved concentration of Benzo[a]pyrene for C_{95} exceeds the maximum concentration limit established by the European Union for drinking water (i.e., $0.01 \text{ } [\mu\text{g/L}]$). This occurs once annually from 2007 to 2009, and remains above the E.U. maximum limit since January 2010 until the end of the study period. In addition, it is observed that the peaks of the series are found in summer but with some displacements towards autumn in comparison to the results for Naphthalene. The mean dissolved concentrations in segment S-9 for the entire study period are $C_{95} = 0.012 \text{ } [\mu\text{g/L}]$, $C_{50} = 0.004 \text{ } [\mu\text{g/L}]$, and $C_{10} = 0.001 \text{ } [\mu\text{g/L}]$.

Similar to Naphthalene, the increase in Benzo(a)pyrene concentrations respond to the increase in discharge effluent from the La Farfana since 2010, as well as the progressive decrease in the streamflow of the Mapocho River since 2009 (Figure 3.4). Lower streamflow means less available water for dilution upstream the WWTP, thus an increasing concentration of PAHs in the river.

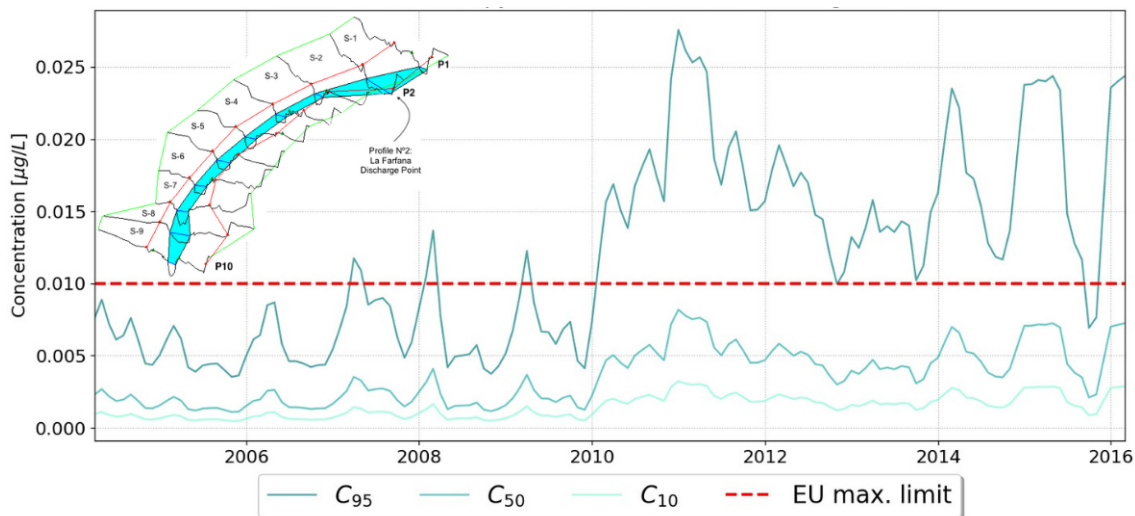


Figure 3.5: Dissolved Benzo[a]pyrene concentration in river segment S-9 (1 km downstream the discharge) for C_{10} , C_{50} and C_{95} . Red dashed line represents the maximum limit for human consumption established by the European Union (i.e., $0.01 \text{ } [\mu\text{g/L}]$).

The sorbed concentrations of B[a]P to TSS were compared to the maximum permissible concentrations (MPCs) in sediments proposed by Verbruggen (2012) and Kalf et al. (1995). Figure 3.8 shows the limit proposed by Kalf et al. ($2,700 \text{ } [\mu\text{g/kg}]$) is exceeded several times for C_{95} . In April 2011, the results for C_{95} , C_{50} and C_{10} exceeded this limit. This may be the result of a month where the Mapocho had low streamflows, high water temperatures, and higher concentrations of B[a]P discharged to the river.

The MPCs proposed by Verbruggen in 2012 for the National Institute for Public Health and the Environment of the Netherlands sets the limit at $490 \text{ } [\mu\text{g/kg}]$, which is the most

stringent limit reported among the reviewed regulations. This limit is exceeded for almost all discharge scenarios. Additionally, the mean sorbed concentrations in S-9 over the entire simulation period are $C_{95} = 1,768 \text{ } [\mu\text{g}/\text{kg}]$, $C_{50} = 821 \text{ } [\mu\text{g}/\text{kg}]$, and $C_{10} = 430 \text{ } [\mu\text{g}/\text{kg}]$.

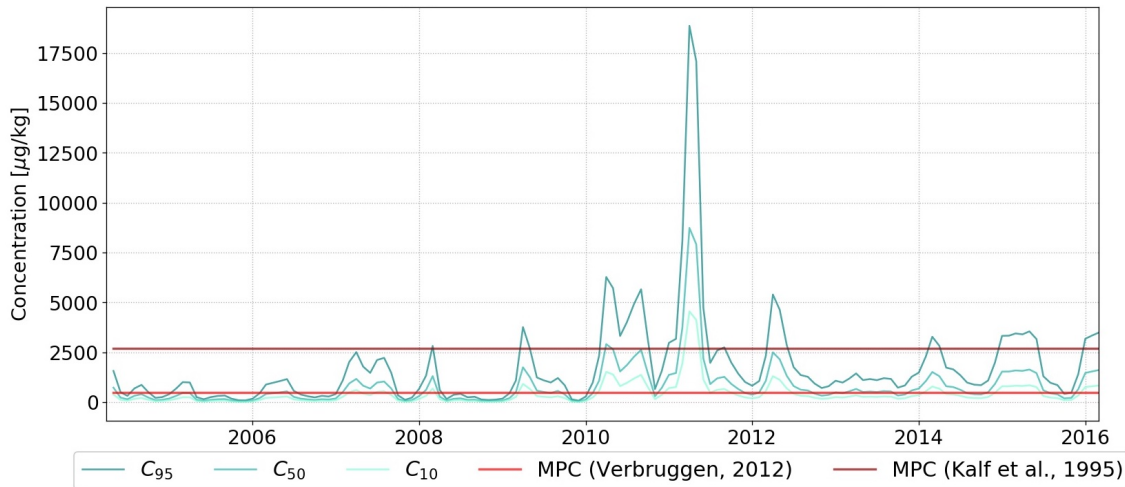


Figure 3.6: Sorbed Benzo[a]pyrene concentration to TSS in river segment S-9 for different percentiles. MCP: Maximum Permissible Concentration for ecosystems.

Figure 3.7 shows the residence time of PAHs for each river segment during November 2005 and January 2011. For November 2005, the streamflow of the Mapocho river was the highest ($50 \text{ } m^3/s$) of the entire period (2004 to 2016) and the average residence of the studied area (S1-S9) was the shortest. In contrast, during January 2011 the Mapocho river was at its lowest streamflow ($10.85 \text{ } m^3/s$), which resulted in the longest average residence time of the entire period. This information is useful when calculating the rate of PAHs partitioning into the sediment and/or gas phases; however, this is out of the scope of the present study.

Regarding the longitudinal profile of the studied area, the longest residence times are found in segment S-2 (i.e., discharge point of La Farfana WWTP), which has the largest cross-sectional area. This area includes an enlarged section of the river, artificially constructed to act as a “buffer” between the river and the WWTP’s discharge point (see Figure D.1), which explains the longest residence time in that stretch of river. The shortest residence times are found in segments S-3 and S-4, which correspond to the segments with the lowest volume of the entire river section evaluated (see Table 3.1). The increase in residence time after segment S-4 agrees with the increase in the average width and cross-sectional areas of each consecutive segment.

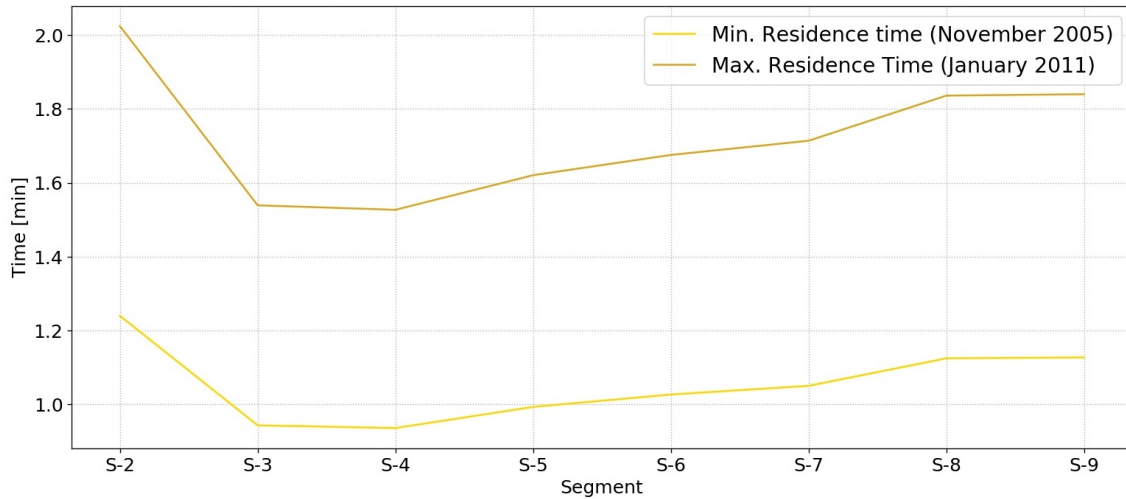


Figure 3.7: Longitudinal distribution by river segment of the residence time of PAHs in the water column, for the dates of highest (January 2011) and lowest (November 2005) residence time in most probable discharge scenario (C_{95}).

Although the residence times are relatively short, as these are highly hydrophobic contaminants, they are expected to volatilize, adhere to solid particles (in the case of Benzo[a]pyrene), and be transported. If transported, the long half-life of the contaminant (more than 200 days) allows it to travel to sites where there is no direct inputs from WWTPs, and eventually bioaccumulate or bio-augment. Although the contribution of WWTPs to PAHs concentrations in rivers is small, the continuous daily input of these pollutants has important environmental effects.

Regarding the waters of the Mapocho River prior to the confluence of the La Farfana discharge, it is possible to expect the presence of PAHs, since two treatment plants discharge upstream of the La Farfana WWTP:

- Arturo Merino Benitez Airport WWTP: With respect to this plant there is no information about its discharges or technical specifications.
- Barrancas WWTP: It's located in the municipality of Pudahuel and meets the demands of the airport business core (ENEA) and is estimated to discharge into the Mapocho River about 5070 m³/day (approximately 0.587 m³/s) (Exempt Resolution No. 242, 2014). This unit, upon entering the Evaluation System through an Environmental Impact Declaration (EID), does not present an Environmental Monitoring Plan and therefore no public information is available on daily effluent flows.

It is important to note that the results presented are only valid when considering only the effluent discharge from the La Farfana plant. The existence of industrial treatment plants upstream of the study area constitutes an unquantified contribution of PAHs to the river that was not included in this study.

Finally, the partition coefficients of the chemicals to solid and to dissolved organic carbon depend on the fraction of organic carbon in the sediment and the magnitude of dissolved

organic carbon in the water, respectively. As no information is available for the latter, and although these are highly site-specific, expected values associated with the characteristics of the Mapocho River, such as its high turbidity, its sandy-silty sediments, and the characteristics of the discharges into the river, were used. However, it is estimated that for future work it is necessary to compare the rivers with dimensionless rivers in order to determine similarities. The use of dimensionless numbers in engineering allows the important task of data reduction of similar problems, which can be a useful guidance for problem simplification due to the lack of information in the Mapocho river.

Chapter 4

Conclusions and recommendations

4.1. Coupled model for PAHs fate in the Mapocho River

The main goal of this work was to implement an integrated modeling framework to evaluate the contributions of La Farfana treatment plant to the fate of two congeners of PAHs (i.e., Nap and B[a]P) in a section of the Mapocho River. Characterizing the existence of these pollutants in the river is imperative to gain insights into the effects they can have on the different trophic and environmental levels. By coupling the HEC-RAS and WASP numerical models, it was possible to incorporate the hydraulic, hydrological, and chemical components that influence the fate of PAHs in the river.

The results obtained show La Farfana WWTP is an important source of PAHs to the Mapocho River. Concerning compliance with maximum limits, all the simulated Nap values were well below the Health Reference Level (HRL) defined by the US-EPA of $140 \mu\text{g/L}$, as most of this pollutant volatilizes. Model simulations showed that B[a]P exceeded the limits established by the EU for drinking water ($0.01 \mu\text{g/L}$) throughout the second half of the study period (2010 onwards) for effluent concentration C_{95} ($0.036 \mu\text{g/L}$). For C_{95} and C_{50} of B[a]P, the fraction of the contaminant sorbed to the river's TSS exceed for almost the entire study period the MPC proposed by Verbruggen in 2012 ($490 [\mu\text{g/kg}]$).

It should be noted that the ultimate responsibility for a model's success lies entirely with the modeler, as WASP just provides a computational framework for the development of a model. The process simplifications in this work are explained by limitations due to data availability. The main limitations include:

- **Availability of WWTP Influent/effluent data:** In general, it is difficult to find measured data of these pollutants in all parts of the world, and there is no reported information in Chile. There are only a few studies conducted that include analysis and measurement of PAHs in other environmental compartments (Section 1.2.1), and they are concentrated in the central-southern part of the country. The lack of quality standards for emerging pollutants in Chile discourages measurements and studies of these pollutants.
- **Availability of river water quality data:** In Chile, available public data is limited to number of parameters of little relevance for the analysis of PAHs fate. Parameters such as TOC and sediment characteristics are key to make accurate predictions and/or fate

simulations for the Mapocho. Even though the presence of persistent organic pollutants in the river are a threat to the health of the ecosystem, there is no reported information about in-situ measurements in the Mapocho. Moreover, the marked seasonal dependence of PAHs concentrations in WWTP's effluents requires they are evaluated by season.

Since sorption into sediments is an important partitioning mechanism for PAHs, it is recommended to include sediment transport in future studies. Also, more segments should be added to cover a larger domain and characterize longitudinal variations in the residence times and processes like sorption and volatilization. Further, the processes of photolysis, biodegradation, and oxidation should be considered in a future application of modeling framework developed in this study. Finally, the concentrations of PAHs should be simulated for climate change scenarios, using projected streamflow time series.

Lastly, the results presented in this study should be interpreted with caution since they are only valid for the section under study. Extrapolation of results for a larger river section is not advised since, for distances > 1 km, more complex processes begin to operate (as photolysis, biodegradation and oxidation), and more data is required to characterize them.

4.2. Effect on *De facto* Reuse

Although a single treatment plant is not enough to generate any impact in the short term, the continuous discharge of effluents (which do not have defined regulations for certain persistent pollutants such as PAHs) supposes an unquantified environmental risk. *De facto* reuse of treated effluents discharged to the Mapocho River is a current practice in Santiago's Metropolitan Area. As has been proven elsewhere, irrigation of crops with water containing PAHs may represent a health risk since PAHs can be absorbed into the plants (Zhang et al., 2017).

From the literature review on international legislation, it is possible to conclude that there is still no consensus in the countries where PAHs are regulated, since the concentrations of permitted discharges are variable and somewhat scarce (Section 1.2.5). Since the European Union presents the most rigorous regulation regarding this pollutant, it is used in this study for comparison. Even though Chilean regulations for PAHs for treated effluents is currently nonexistent, this study provides a range of PAHs effluent concentrations based on actual measured data around the world. This information can be quite useful for future studies related to fate analysis and regulatory contaminant limits.

It is expected that, under scenarios of decreasing streamflow in the Mapocho River due to climate change, the concentrations of PAHs in the water will be increasingly higher. The Mapocho River, as one of the important sources of irrigation water for the Metropolitan Region, it is also candidate for potable water reuse. Future examinations of extreme events are also recommended, since increasing streamflow may resuspend sediments already deposited in the river and transport them long distances, eventually reaching the sea.

The impacts of emerging pollutants on aquatic ecosystems can affect the different trophic levels, urging the consideration of environmental quality standards (NSCA, for its acronym

in Spanish). NSCAs are developed and implemented to protect aquatic ecosystems and also, indirectly, their ecosystem services. The biggest challenge of the NSCAs is to address the control of emerging contaminants, such as PAHs and PCBs, among others. Thus, in addition to showing the current state of research of these pollutants in Chile, this work seeks to call on the regulators of water quality standards to lead research processes aimed at building an inventory of emerging pollutants that may be found in the local context.

Bibliography

- Abdel-Shafy, H. I., & Mansour, M. S. (2016). A review on polycyclic aromatic hydrocarbons: Source, environmental impact, effect on human health and remediation. *Egyptian Journal of Petroleum*, 25(1), 107–123. Retrieved from <http://dx.doi.org/10.1016/j.ejpe.2015.03.011> doi: 10.1016/j.ejpe.2015.03.011
- Adeniji, A. O., Okoh, O. O., & Okoh, A. I. (2019). Distribution pattern and health risk assessment of polycyclic aromatic hydrocarbons in the water and sediment of Algoa Bay, South Africa. *Environmental Geochemistry and Health*, 41(3), 1303–1320. Retrieved from <https://doi.org/10.1007/s10653-018-0213-x> doi: 10.1007/s10653-018-0213-x
- Agency for Toxic Substances and Disease Registry. (1995). *Toxicological profile for polycyclic aromatic hydrocarbons* (Tech. Rep.). Retrieved from <https://www.atsdr.cdc.gov/toxprofiles/tp69-c5.pdf>
- Alvarez-Garretton, C., Mendoza, P. A., Pablo Boisier, J., Addor, N., Galleguillos, M., Zambrano-Bigiarini, M., ... Ayala, A. (2018). The CAMELS-CL dataset: Catchment attributes and meteorology for large sample studies-Chile dataset. *Hydrology and Earth System Sciences*, 22(11), 5817–5846. doi: 10.5194/hess-22-5817-2018
- Ambrose, B. H. Y. K. C. W. T., B.; Avant. (2017). Water Quality Assessment Simulation Program (WASP8): Upgrades to the Advanced Toxicant Module for Simulating Dissolved Chemicals, Nanomaterials, and Solids. (September), 49. Retrieved from https://cfpub.epa.gov/si/si_public_record_report.cfm?Lab=NERL&dirEntryId=338180
- Ambrose, R. B., & Wool, T. A. (2017). WASP8 Stream Transport - Model Theory and User's Guide. , 1–67. Retrieved from <https://www.epa.gov/sites/production/files/2018-05/documents/stream-transport-user-guide.pdf>
- ATSDR. (2019). *ATSDR 2019 substance priority list*. Retrieved from <https://www.atsdr.cdc.gov/spl/index.html>
- Azouzi, R., Charef, A., zaghdoudi, S., Khadhar, S., Shabou, N., Boughanmi, H., ... Hajjaj, S. (2016). Effect of long-term irrigation with treated wastewater of three soil types on their bulk densities, chemical properties and PAHs content in semi-arid climate. *Arabian Journal of Geosciences*, 9(1), 1–13. doi: 10.1007/s12517-015-2085-z
- Baek, S. O., Field, R. A., Goldstone, M. E., Kirk, P. W., Lester, J. N., & Perry, R. (1991). A review of atmospheric polycyclic aromatic hydrocarbons: Sources, fate and behavior. *Water, Air, and Soil Pollution*, 60(3), 279–300. Retrieved from <https://doi.org/10.1007/BF00282628> doi: 10.1007/BF00282628

- Bahadur, R., Amstutz, D. E., & Samuels, W. B. (2013). Water Contamination Modeling—A Review of the State of the Science. *Journal of Water Resource and Protection*, 05(02), 142–155. Retrieved from <http://www.scirp.org/journal/doi.aspx?DOI=10.4236/jwarp.2013.52016> doi: 10.4236/jwarp.2013.52016
- Barnes, H. (1969). Roughness characteristics of natural channels. *Journal of Hydrology*, 7(3), 354. doi: 10.1016/0022-1694(69)90113-9
- Barra, R., Popp, P., Quiroz, R., Treutler, H. C., Araneda, A., Bauer, C., & Urrutia, R. (2006). Polycyclic aromatic hydrocarbons fluxes during the past 50 years observed in dated sediment cores from Andean mountain lakes in central south Chile. *Ecotoxicology and Environmental Safety*, 63(1), 52–60. doi: 10.1016/j.ecoenv.2005.07.025
- Bastian, R., & Murray, D. (2012). *2012 Guidelines for Water Reuse* (Tech. Rep.). Washington, DC: US EPA Office of Research and Development. Retrieved from <http://nepis.epa.gov/Adobe/PDF/P100FS7K.pdf>
- Bowman, J. C., Zhou, J. L., & Readman, J. W. (2002). Sorption and desorption of benzo(a)pyrene in aquatic systems. *Journal of Environmental Monitoring*, 4(5), 761–766. doi: 10.1039/b204969b
- Bravo-Linares, C., Ovando-Fuentealba, L., Mudge, S. M., Cerpa, J., & Loyola-Sepulveda, R. (2012). Source Allocation of Aliphatic and Polycyclic Aromatic Hydrocarbons in Particulate-Phase (PM 10) in the City of Valdivia, Chile. *Polycyclic Aromatic Compounds*, 32(3), 390–407. doi: 10.1080/10406638.2012.661829
- Bravo-Linares, C., Ovando-Fuentealba, L., Orellana-Donoso, S., Villenas-Fernández, K., Hernández-Millán, M., Mudge, S. M., ... Loyola-Sepulveda, R. (2017). Source Apportionment of PAHs in Airborne Particulates (PM2.5) in Southern Chile. *Polycyclic Aromatic Compounds*, 37(2-3), 189–202. doi: 10.1080/10406638.2016.1238400
- Brazilian Ministry of Health, R. F. d. B. (2004). Ordenanza nº 518: Establece los procedimientos y responsabilidades relativos al control y la vigilancia de la calidad del agua para consumo humano y su norma de potabilidad, y establece otras disposiciones [Computer software manual]. Retrieved from http://189.28.128.100/dab/docs/legislacao/portaria518_25_03_04.pdf
- Brunner, G. W. (2016). HEC-RAS River Analysis System User's Manual. US Army Corps of Engineers–Hydrologic Engineering Center. (January), 1–790. Retrieved from <https://www.hec.usace.army.mil/software/hec-ras/documentation/HEC-RAS5.0UsersManual.pdf>
- Burkhard, L. P. (2000). Estimating dissolved organic carbon partition coefficients for nonionic organic chemicals. *Environmental Science and Technology*, 34(22), 4663–4668. doi: 10.1021/es001269l
- Busetti, F., Heitz, A., Cuomo, M., Badoer, S., & Traverso, P. (2006). Determination of sixteen polycyclic aromatic hydrocarbons in aqueous and solid samples from an Italian wastewater treatment plant. *Journal of Chromatography A*, 1102(1-2), 104–115. doi: 10.1016/j.chroma.2005.10.013

- Cerniglia, C. E. (1992). Biodegradation of polycyclic aromatic hydrocarbons. *Biodegradation*, 3(2-3), 351–368. Retrieved from <http://link.springer.com/10.1007/BF00129093> doi: 10.1007/BF00129093
- Chiou, C. T., McGroddy, S. E., & Kile, D. E. (1998). Partition characteristics of polycyclic aromatic hydrocarbons on soils and sediments. *Environmental Science and Technology*, 32(2), 264–269. doi: 10.1021/es970614c
- Chow, V. T. (1959). *Open-Channel Hydraulics*. McGraw-Hill.
- Crossette, M. P. C. K. Y. M. M., E. (2015). Application of BASINS/HSPF to Data-scarce Watersheds. (February), 88. Retrieved from <https://www.epa.gov/ceam/hydrological-simulation-program-fortran-hspf#Application>
- Das, S., Raj, R., Mangwani, N., Dash, H. R., & Chakraborty, J. (2014). 2 - Heavy Metals and Hydrocarbons: Adverse Effects and Mechanism of Toxicity. In S. B. T. M. B. Das & Bioremediation (Eds.), (pp. 23–54). Oxford: Elsevier. Retrieved from <http://www.sciencedirect.com/science/article/pii/B9780128000212000029> doi: <https://doi.org/10.1016/B978-0-12-800021-2.00002-9>
- Dirección General de Aguas de Chile. (2004). *Diagnóstico y clasificación de los Cursos y cuerpos de agua Según objetivos de calidad. Cuenca del Rio Maipo* (Tech. Rep.). Retrieved from <https://mma.gob.cl/wp-content/uploads/2017/12/Maipo.pdf>
- Di Toro, D. M., Fitzpatrick, J. J., Thomann, R. V., & Hydrosience, I. (1983). Documentation For Water Quality Analysis Simulation Program (WASP) And Model Verification Program (MVP). *Proc Spie*, 34(5), 4–10.
- Eisler, R. (1987). *Polycyclic aromatic hydrocarbon hazards to fish, wildlife, and invertebrates: a synoptic review* (No. 11). Fish and Wildlife Service, US Department of the Interior.
- EUR-Lex. (2006). *Regulation (ec) no 1907/2006 of the european parliament and of the council on the registration, evaluation, authorisation and restriction of chemicals (reach) as regards polycyclic aromatic hydrocarbons* (Tech. Rep.). Comission Regulation - European Union. Retrieved from <https://eur-lex.europa.eu/legal-content/EN/TXT/?qid=1595207811024&uri=CELEX:32013R1272>
- Fatone, F., Di Fabio, S., Bolzonella, D., & Cecchi, F. (2011). Fate of aromatic hydrocarbons in Italian municipal wastewater systems: An overview of wastewater treatment using conventional activated-sludge processes (CASP) and membrane bioreactors (MBRs). *Water Research*, 45(1), 93–104. Retrieved from <http://dx.doi.org/10.1016/j.watres.2010.08.011> doi: 10.1016/j.watres.2010.08.011
- Fischer, H. B., List, E. J., Koh, R. C., Imberger, J., & Brooks, N. H. (1979). Mixing in Rivers. In *Mixing in inland and coastal waters* (pp. 104–147). San Diego: Elsevier. Retrieved from <http://www.sciencedirect.com/science/article/pii/B978008051177150009X><https://linkinghub.elsevier.com/retrieve/pii/B978008051177150009X> doi: 10.1016/B978-0-08-051177-1.50009-X

- Forsgren, A. J. (2015). *Wastewater treatment: Occurrence and fate of polycyclic aromatic hydrocarbons (PAHs)*.
- González Sepúlveda, E., Loyola Sepúlveda, R., Neira Hinojosa, J., & Neira González, F. (2013). Contenido, distribución y origen de hidrocarburos en sedimentos de tres lagunas urbanas de Concepción - Chile. *Química Nova*, *36*(5), 669–674. Retrieved from http://www.scielo.br/scielo.php?script=sci_arttext&pid=S0100-40422013000500010&lng=es&nrm=iso&tlng=en doi: 10.1590/S0100-40422013000500010
- Haddaoui, I., Mahjoub, O., Mahjoub, B., Boujelben, A., & Di Bella, G. (2016). Occurrence and distribution of PAHs, PCBs, and chlorinated pesticides in Tunisian soil irrigated with treated wastewater. *Chemosphere*, *146*, 195–205. Retrieved from <http://dx.doi.org/10.1016/j.chemosphere.2015.12.007> doi: 10.1016/j.chemosphere.2015.12.007
- Hattemer-Frey, H. A., & Travis, C. C. (1991, 5). Benzo-a-Pyrene: Environmental Partitioning and Human Exposure. *Toxicology and Industrial Health*, *7*(3), 141–157. Retrieved from <http://journals.sagepub.com/doi/10.1177/074823379100700303> doi: 10.1177/074823379100700303
- Hussain, K., Hoque, R. R., Balachandran, S., Medhi, S., Idris, M. G., Rahman, M., & Hussain, F. L. (2019). *Monitoring and Risk Analysis of PAHs in the Environment*. doi: 10.1007/978-3-319-73645-7{_}29
- IARC. (2010). Some Non-heterocyclic Polycyclic Aromatic Hydrocarbons and Some Related Exposures. In *Iarc monographs on the evaluation of carcinogenic risks to humans* (Vol. 92, pp. 1–819). Lyon: International Agency for Research on Cancer. Retrieved from <http://jcp.bmj.com/cgi/doi/10.1136/jcp.48.7.691-a>
- Jaco, R. (2020). *Evaluación del efecto de las contribuciones de plantas de tratamiento en las concentraciones de PCBs del río Mapocho, Chile*. (Unpublished doctoral dissertation). Tesis para optar al grado de Magister en Ciencias de la Ingeniería mención Recursos y Medio Ambiente Hídrico. Departamento de Ingeniería Civil. Universidad de Chile.
- Kalf, D. F., Crommentuijn, T., & Van de Plassche, E. J. (1997). Environmental quality objectives for 10 polycyclic aromatic hydrocarbons (PAHS). *Ecotoxicology and Environmental Safety*, *36*(1), 89–97. doi: 10.1006/eesa.1996.1495
- Khairy, M. A., Weinstein, M. P., & Lohmann, R. (2014). Trophodynamic behavior of hydrophobic organic contaminants in the aquatic food web of a tidal river. *Environmental Science and Technology*, *48*(21), 12533–12542. doi: 10.1021/es502886n
- Knightes, C. D., Avant, B., Han, Y., Bouchard, D. C., Zepp, R., Wool, T., ... States, U. (2020). EPA Public Access. , 1–35. doi: 10.1016/j.envsoft.2018.10.012.Modeling
- Koormann, F., Rominger, J., Schowanek, D., Wagner, J. O., Schröder, R., Wind, T., ... Whelan, M. J. (2006). Modeling the fate of down-the-drain chemicals in rivers: An improved software for GREAT-ER. *Environmental Modelling and Software*, *21*(7), 925–936. doi: 10.1016/j.envsoft.2005.04.009

- Lawal, A. T. (2017, 1). Polycyclic aromatic hydrocarbons. A review. *Cogent Environmental Science*, 3(1), 1339841. Retrieved from <https://doi.org/10.1080/23311843.2017.1339841> doi: 10.1080/23311843.2017.1339841
- Li, J., Dong, H., Zhang, D., Han, B., Zhu, C., Liu, S., ... Li, X. (2015). Sources and ecological risk assessment of PAHs in surface sediments from Bohai Sea and northern part of the Yellow Sea, China. *Marine Pollution Bulletin*, 96(1-2), 485–490. Retrieved from <http://dx.doi.org/10.1016/j.marpolbul.2015.05.002> doi: 10.1016/j.marpolbul.2015.05.002
- Liu, Z., Li, Q., Wu, Q., Kuo, D. T., Chen, S., Hu, X., ... Luo, M. (2017). Removal efficiency and risk assessment of polycyclic aromatic hydrocarbons in a typical municipal wastewater treatment facility in Guangzhou, China. *International Journal of Environmental Research and Public Health*, 14(8). doi: 10.3390/ijerph14080861
- Mackay, D., Paterson, S., & Joy, M. (1983). A quantitative water, air, sediment interaction (QWASI) fugacity model for describing the fate of chemicals in rivers. *Chemosphere*, 12(9-10), 1193–1208. doi: 10.1016/0045-6535(83)90125-X
- Man, Y. B., Chow, K. L., Cheng, Z., Mo, W. Y., Chan, Y. H., Lam, J. C. W., ... Wong, M. H. (2017). Profiles and removal efficiency of polycyclic aromatic hydrocarbons by two different types of sewage treatment plants in Hong Kong. *Journal of Environmental Sciences (China)*, 53, 196–206. Retrieved from <http://dx.doi.org/10.1016/j.jes.2016.04.020> doi: 10.1016/j.jes.2016.04.020
- Manoli, E., & Samara, C. (1999). Occurrence and Mass Balance of Polycyclic Aromatic Hydrocarbons in the Thessaloniki Sewage Treatment Plant. *Journal of Environmental Quality*, 28(1), 176–187. doi: 10.2134/jeq1999.00472425002800010021x
- Muñoz, C., Droppelmann, A., Erazo, M., Aceituno, P., Orellana, C., Parro, J., ... Iglesias, V. (2016). Occupational exposure to polycyclic aromatic hydrocarbons: A cross-sectional study in bars and restaurants in Santiago, Chile. *American Journal of Industrial Medicine*, 59(10), 887–896. doi: 10.1002/ajim.22616
- Nas, B., Argun, M., Dolu, T., Ateş, H., Yel, E., Koyuncu, S., ... Kara, M. (2020, 8). Occurrence, loadings and removal of EU-priority polycyclic aromatic hydrocarbons (PAHs) in wastewater and sludge by advanced biological treatment, stabilization pond and constructed wetland. *Journal of Environmental Management*, 268(April), 110580. Retrieved from <https://linkinghub.elsevier.com/retrieve/pii/S0301479720305132> doi: 10.1016/j.jenvman.2020.110580
- National Center for Biotechnology Information. (2021a). *PubChem Compound Summary for CID 2336, Benzo[a]pyrene*. Retrieved from https://pubchem.ncbi.nlm.nih.gov/compound/Benzo_a_pyrene
- National Center for Biotechnology Information. (2021b). *PubChem Compound Summary for CID 931, Naphthalene*. Retrieved from <https://pubchem.ncbi.nlm.nih.gov/compound/Naphthalene>
- Ozaki, N., Takamura, Y., Kojima, K., & Kindaichi, T. (2015). Loading and removal of PAHs in a wastewater treatment plant in a separated sewer system. *Water Research*, 80,

- 337–345. Retrieved from <http://dx.doi.org/10.1016/j.watres.2015.05.002> doi: 10.1016/j.watres.2015.05.002
- Park, R. A., Clough, J. S., & Wellman, M. C. (2008). AQUATOX: Modeling environmental fate and ecological effects in aquatic ecosystems. *Ecological Modelling*, *213*(1), 1–15. doi: 10.1016/j.ecolmodel.2008.01.015
- Pham, T. T., & Proulx, S. (1997). PCBs and PAHs in the Montreal urban community (Quebec, Canada) wastewater treatment plant and in the effluent plume in the St Lawrence river. *Water Research*, *31*(8), 1887–1896. doi: 10.1016/S0043-1354(97)00025-0
- Pozo, K., Estellano, V. H., Harner, T., Diaz-Robles, L., Cereceda-Balic, F., Etcharren, P., ... Vergara-Fernández, A. (2015). Assessing Polycyclic Aromatic Hydrocarbons (PAHs) using passive air sampling in the atmosphere of one of the most wood-smoke-polluted cities in Chile: The case study of Temuco. *Chemosphere*, *134*, 475–481. Retrieved from <http://dx.doi.org/10.1016/j.chemosphere.2015.04.077> doi: 10.1016/j.chemosphere.2015.04.077
- Pozo, K., Harner, T., Rudolph, A., Oyola, G., Estellano, V. H., Ahumada-Rudolph, R., ... Focardi, S. (2012). Survey of persistent organic pollutants (POPs) and polycyclic aromatic hydrocarbons (PAHs) in the atmosphere of rural, urban and industrial areas of Concepcin, Chile, using passive air samplers. *Atmospheric Pollution Research*, *3*(4), 426–434. Retrieved from <http://dx.doi.org/10.5094/APR.2012.049> doi: 10.5094/APR.2012.049
- Pozo, K., Perra, G., Menchi, V., Urrutia, R., Parra, O., Rudolph, A., & Focardi, S. (2011). Levels and spatial distribution of polycyclic aromatic hydrocarbons (PAHs) in sediments from Lengua Estuary, central Chile. *Marine Pollution Bulletin*, *62*(7), 1572–1576. Retrieved from <http://dx.doi.org/10.1016/j.marpolbul.2011.04.037> doi: 10.1016/j.marpolbul.2011.04.037
- Qi, W., Liu, H., Pernet-Coudrier, B., & Qu, J. (2013). Polycyclic aromatic hydrocarbons in wastewater, WWTPs effluents and in the recipient waters of Beijing, China. *Environmental Science and Pollution Research*, *20*(6), 4254–4260. doi: 10.1007/s11356-012-1435-6
- Qian, X., Liang, B., Fu, W., Liu, X., & Cui, B. (2016). Polycyclic aromatic hydrocarbons (PAHs) in surface sediments from the intertidal zone of Bohai Bay, Northeast China: Spatial distribution, composition, sources and ecological risk assessment. *Marine Pollution Bulletin*, *112*(1-2), 349–358. Retrieved from <http://dx.doi.org/10.1016/j.marpolbul.2016.07.040> doi: 10.1016/j.marpolbul.2016.07.040
- Qiao, M., Qi, W., Liu, H., & Qu, J. (2014a). Occurrence, behavior and removal of typical substituted and parent polycyclic aromatic hydrocarbons in a biological wastewater treatmentplant. *Water Research*, *52*(February), 11–19. Retrieved from <http://dx.doi.org/10.1016/j.watres.2013.12.032> doi: 10.1016/j.watres.2013.12.032
- Qiao, M., Qi, W., Liu, H., & Qu, J. (2014b). Occurrence, behavior and removal of typical substituted and parent polycyclic aromatic hydrocarbons in a biological wastewater treatmentplant. *Water Research*, *52*, 11–19. doi: 10.1016/j.watres.2013.12.032
- Qiao, M., Qi, W., Liu, H., & Qu, J. (2014c). Oxygenated, nitrated, methyl and parent polycyclic aromatic hydrocarbons in rivers of Haihe River System, China: Occurrence, possible

formation, and source and fate in a water-shortage area. *Science of the Total Environment*, 481(1), 178–185. Retrieved from <http://dx.doi.org/10.1016/j.scitotenv.2014.02.050> doi: 10.1016/j.scitotenv.2014.02.050

Rengarajan, T., Rajendran, P., Nandakumar, N., Lokeshkumar, B., Rajendran, P., & Nishigaki, I. (2015). Exposure to polycyclic aromatic hydrocarbons with special focus on cancer. *Asian Pacific Journal of Tropical Biomedicine*, 5(3), 182–189. Retrieved from [http://dx.doi.org/10.1016/S2221-1691\(15\)30003-4](http://dx.doi.org/10.1016/S2221-1691(15)30003-4) doi: 10.1016/S2221-1691(15)30003-4

Sánchez-Avila, J., Bonet, J., Velasco, G., & Lacorte, S. (2009). Determination and occurrence of phthalates, alkylphenols, bisphenol A, PBDEs, PCBs and PAHs in an industrial sewage grid discharging to a Municipal Wastewater Treatment Plant. *Science of the Total Environment*, 407(13), 4157–4167. Retrieved from <http://dx.doi.org/10.1016/j.scitotenv.2009.03.016> doi: 10.1016/j.scitotenv.2009.03.016

Shi, B., Nguелеu, S. K., Rezanezhad, F., Slowinski, S., Pronk, G. J., Smeaton, C. M., ... Van Cappellen, P. (2020). Sorption and Desorption of the Model Aromatic Hydrocarbons Naphthalene and Benzene: Effects of Temperature and Soil Composition. *Frontiers in Environmental Chemistry*, 1, 13. Retrieved from <https://www.frontiersin.org/article/10.3389/fenvc.2020.581103> doi: 10.3389/fenvc.2020.581103

Sienra, M. d. R., Rosazza, N. G., & Préndez, M. (2005). Polycyclic aromatic hydrocarbons and their molecular diagnostic ratios in urban atmospheric respirable particulate matter. *Atmospheric Research*, 75(4), 267–281. doi: 10.1016/j.atmosres.2005.01.003

Song, X., Hu, X., He, M., Liang, R., Li, Y., & Li, F. (2013). Distribution and sources of polycyclic aromatic hydrocarbons in the surface water of Taizi River, Northeast of China. *Environmental Monitoring and Assessment*, 185(10), 8375–8382. doi: 10.1007/s10661-013-3179-2

Srogi, K. (2007). Monitoring of environmental exposure to polycyclic aromatic hydrocarbons: A review. *Environmental Chemistry Letters*, 5(4), 169–195. doi: 10.1007/s10311-007-0095-0

Sun, S., Jia, L., Li, B., Yuan, A., Kong, L., Qi, H., ... Wu, Y. (2018). The occurrence and fate of PAHs over multiple years in a wastewater treatment plant of Harbin, Northeast China. *Science of the Total Environment*, 624, 491–498. doi: 10.1016/j.scitotenv.2017.12.029

Tian, W., Bai, J., Liu, K., Sun, H., & Zhao, Y. (2012a). Occurrence and removal of polycyclic aromatic hydrocarbons in the wastewater treatment process. *Ecotoxicology and Environmental Safety*, 82, 1–7. Retrieved from <http://dx.doi.org/10.1016/j.ecoenv.2012.04.020> doi: 10.1016/j.ecoenv.2012.04.020

Tian, W., Bai, J., Liu, K., Sun, H., & Zhao, Y. (2012b). Occurrence and removal of polycyclic aromatic hydrocarbons in the wastewater treatment process. *Ecotoxicology and Environmental Safety*, 82, 1–7. Retrieved from <http://dx.doi.org/10.1016/j.ecoenv.2012.04.020> doi: 10.1016/j.ecoenv.2012.04.020

- Undersecretary of Water Resources of Argentina, R. A. (2003). Niveles guía nacionales de calidad de agua ambiente: Benzo[a]pireno [Computer software manual]. Retrieved from <https://www.argentina.gob.ar/sites/default/files/documento22.pdf>
- U.S. Environmental Protection Agency. (2003). *Contaminant Candidate List Regulatory Determination Support Document for Naphthalene* (Tech. Rep.). US-EPA. Retrieved from https://www.epa.gov/sites/production/files/2014-09/documents/support_cc1_naphthalene_ccl_regdet.pdf
- USDHHS/PHS/NTP. (2016). *Report on carcinogens*. Retrieved from https://ntp.niehs.nih.gov/ntp/roc/content/listed_substances_508.pdf
- US-EPA. (2011). *Priority pollutants* (Tech. Rep.). U.S. Environmental Protection Agency. Retrieved from <http://water.epa.gov/scitech/methods/cwa/pollutants.cfm>
- US-EPA. (2020). National primary drinking water regulations. Retrieved from <https://www.epa.gov/ground-water-and-drinking-water/national-primary-drinking-water-regulations>
- Verbruggen, E. (2012). *Environmental risk limits for polycyclic aromatic hydrocarbons (PAHs): For direct aquatic, benthic, and terrestrial toxicity* (Tech. Rep.). Bilthoven (NL): National Institute for Public Health and the Environment. Retrieved from <https://www.rivm.nl/bibliotheek/rapporten/607711007.pdf>
- Vogelsang, C., Grung, M., Jantsch, T. G., Tollefsen, K. E., & Liltved, H. (2006). Occurrence and removal of selected organic micropollutants at mechanical, chemical and advanced wastewater treatment plants in Norway. *Water Research*, *40*(19), 3559–3570. doi: 10.1016/j.watres.2006.07.022
- Wang, C., Feng, Y., Sun, Q., Zhao, S., Gao, P., & Li, B. L. (2012). A multimedia fate model to evaluate the fate of PAHs in Songhua River, China. *Environmental Pollution*, *164*, 81–88. Retrieved from <http://dx.doi.org/10.1016/j.envpol.2012.01.025> doi: 10.1016/j.envpol.2012.01.025
- Wang, W., Massey Simonich, S. L., Giri, B., Xue, M., Zhao, J., Chen, S., . . . Tao, S. (2011). Spatial distribution and seasonal variation of atmospheric bulk deposition of polycyclic aromatic hydrocarbons in Beijing-Tianjin region, North China. *Environmental Pollution*, *159*(1), 287–293. Retrieved from <http://dx.doi.org/10.1016/j.envpol.2010.08.029> doi: 10.1016/j.envpol.2010.08.029
- Wang, X., Xi, B., Huo, S., Sun, W., Pan, H., Zhang, J., . . . Liu, H. (2013). Characterization, treatment and releases of PBDEs and PAHs in a typical municipal sewage treatment plant situated beside an urban river, East China. *Journal of Environmental Sciences (China)*, *25*(7), 1281–1290. Retrieved from [http://dx.doi.org/10.1016/S1001-0742\(12\)60201-0](http://dx.doi.org/10.1016/S1001-0742(12)60201-0) doi: 10.1016/S1001-0742(12)60201-0
- WaterReuse Association. (2017). Water Reuse Terminology. Retrieved from <https://watereuse.org/educate/water-reuse-101/glossary/>

- WHO. (2000). Air Quality Guidelines : Polycyclic aromatic hydrocarbons. *Air Quality Guidelines : Polycyclic aromatic hydrocarbons*, 1, 1–24. Retrieved from http://www.euro.who.int/__data/assets/pdf_file/0015/123063/AQG2ndEd_5_9PAH.pdf
- Wilks, D. S. (2011). *Statistical Methods in the Atmospheric Sciences*. Elsevier Science. Retrieved from <https://books.google.cl/books?id=IJuCVtQ0ySIC>
- Wlodarczyk-Makula, M. (2005). The loads of PAHs in wastewater and sewage sludge of municipal treatment plant. *Polycyclic Aromatic Compounds*, 25(2), 183–194. doi: 10.1080/10406630590930743
- Zelinkova, Z., & Wenzl, T. (2015). The Occurrence of 16 EPA PAHs in Food – A Review. *Polycyclic Aromatic Compounds*, 35(2-4), 248–284. doi: 10.1080/10406638.2014.918550
- Zhang, S., Yao, H., Lu, Y., Yu, X., Wang, J., Sun, S., ... Zhang, D. (2017). Uptake and translocation of polycyclic aromatic hydrocarbons (PAHs) and heavy metals by maize from soil irrigated with wastewater. *Scientific Reports*, 7(1), 1–11. Retrieved from <http://dx.doi.org/10.1038/s41598-017-12437-w> doi: 10.1038/s41598-017-12437-w
- Zheng, B., Ma, Y., Qin, Y., Zhang, L., Zhao, Y., Cao, W., ... Han, C. (2016). Distribution, sources, and risk assessment of polycyclic aromatic hydrocarbons (PAHs) in surface water in industrial affected areas of the Three Gorges Reservoir, China. *Environmental Science and Pollution Research*, 23(23), 23485–23495. Retrieved from <http://dx.doi.org/10.1007/s11356-016-7524-1> doi: 10.1007/s11356-016-7524-1

Appendix A

WASP8 Model Equations

A.1. General Aspects of the Model

The version of the model to be used is number eight. The hydrodynamics can be of impermanent or permanent regime. In this case, it is used in a permanent regime and the reaction rates are not necessarily uniform along the section under study. The WASP model has the following characteristics:

- **Software and graphical interface:** WASP8 model interface is implemented using the Microsoft Windows operating system.
- **Spatial resolution:** Model simulates flows in 1, 2, and 3 dimensions.
- **Segmentation:** River is divided into sections or segments and these represent the longitudinal component to be modeled.
- **Hydrodynamics:** Flow of steady or unsteady state.
- **Flow transport:** Water column flow is input via transport field 1. Circulation patterns may be described using one of the available flow options, which can be grouped into two transport options.
 - **Descriptive flow:** Flow Routing or Stream Routing. The outflow from a descriptive flow segment is equal to the sum of the inflows to that segment.
 - **Kinematic wave stream:** Kinematic flow is controlled by bottom slope and bottom roughness.
- **Heat balance:** Temperature and heat balance are dynamically simulated as a function of the intra-daily variation of meteorological variables (e.g. air temperature, wind speed, atmospheric pressure).
- **Daily water quality kinetics:** Water quality variables are dynamically simulated on an hourly, daily, or monthly scale.
- **Modules:** WASP8 includes two modules for water quality, “Advanced Toxicant” for toxicants and “Advanced Eutrophication” for conventional water quality. To simulate organic pollutants such as PAHs, the advanced toxicant module is used. A detailed description of this module is given in Appendix A.9.

A.2. Governing Flow Equations

The WASP streamflow model consists of a set of one-dimensional equations solving water flow and water volume in a branching stream or shallow river network. This network can include free-flowing stream reaches (kinematic wave flow), ponded reaches (weir overflow), and backwater or tidally influenced reaches (dynamic flow). The equation of motion, based on the conservation of momentum, predicts water velocities and flows. The equation of continuity, based on the conservation of volume, predicts water heights (heads) and volumes. The one-dimensional continuity equation is given by:

$$\frac{\partial Q}{\partial t} + \frac{\partial A}{\partial x} = 0 \quad (\text{A.1})$$

where Q is volumetric flow, [m^3/sec] and A is cross-sectional area [m^2]. For rectangular channels, where width is constant, Equation A.1 becomes:

$$\frac{\partial Q}{\partial t} + B \frac{\partial H}{\partial x} = 0 \quad (\text{A.2})$$

where B is channel width [m] and H is water surface elevation [m]. The equations of motion implemented in kinematic flow reaches (the selected reach in this study) are described in the following section.

A.3. Kinematic wave flow

For one-dimensional, free-flowing stream reaches, kinematic wave flow routing is a simple but realistic option to drive advective transport. The kinematic wave equation calculates flow wave propagation and resulting variations in flows, velocities, widths, and depths throughout a stream network. This well-known equation is a solution of the onedimensional continuity equation and a simplified form of the momentum equation that considers the effects of gravity and friction:

$$g(S_0 - S_f) = 0 \quad (\text{A.3})$$

where g is acceleration of gravity [m/sec^2], S_0 is the bottom slope, and S_f is the friction slope. Manning's equation expresses the friction force as a function of water velocity and hydraulic radius:

$$S_f = \frac{n^2 v^2}{R^{4/3}} \quad (\text{A.4})$$

where n is the Manning friction factor, v is water velocity [m/sec], and R is hydraulic radius [m], which is equivalent to the cross-sectional average depth, D . From the simplified momentum equation, S_0 can be equated to S_f . Hydraulic radius can be expressed as cross-sectional area divided by width, B [m]. Substituting these into the Manning's equation and rearranging terms gives flow as a function of bottom slope, cross-sectional area, and width:

$$Q = \frac{1}{n} \frac{A^{5/3}}{B^{2/3}} S_o^{1/2} \quad (\text{A.5})$$

Substituting this expression into the continuity equation and differentiating A with respect

to time gives the kinematic wave differential equation:

$$\frac{\partial Q}{\partial x} + \alpha\beta Q^{\beta-1} \cdot \frac{\partial Q}{\partial t} = 0 \quad (\text{A.6})$$

where, for rectangular channels:

$$\alpha = \left(\frac{nB^{2/3}}{S_f} \right)^{3/5}, \quad \beta = 3/5 \quad (\text{A.7})$$

A.4. The model transport scheme

Transport includes advection and dispersion of water quality constituents. Advection and dispersion in WASP are each divided into six distinct types, or "fields." In this work it is used the first transport field, involving advective flow and dispersive mixing in the water column. Advective flow carries water quality constituents "downstream" with the water and accounts for instream dilution. Dispersion causes further mixing and dilution between regions of high concentrations and regions of low concentrations.

The second transport field specifies the movement of pore water in the sediment bed. Dissolved water quality constituents are carried through the bed by pore water flow and are exchanged between the bed and the water column by pore water diffusion. The third, fourth, and fifth transport fields specify the transport of particulate pollutants by the settling, resuspension, and sedimentation of solids. Water quality constituents sorbed onto solid particles are transported between the water column and the sediment bed. The three solids fields can be defined by the user as size fractions, such as sand, silt, and clay, or as inorganic, phytoplankton, and organic solids. The sixth transport field represents evaporation or precipitation from or to surface water segments.

A.5. Water Column Dispersion

Dispersive water column exchanges significantly influence the transport of dissolved and particulate pollutants in such water bodies like lakes, reservoirs, and estuaries. Even in rivers, longitudinal dispersion can be the most important process diluting peak concentrations that may result from unsteady loads or spills. In WASP8, water column dispersion is input and several groups of exchanges may be defined by the user. For each group, the user must supply a time function giving dispersion coefficient values (in m²/sec) as they vary in time. For each exchange in the group, the user must supply an interfacial area, a characteristic mixing length, and the adjoining segments between which the exchange takes place. The characteristic mixing length is typically the distance between the segment midpoints. The interfacial area is the area normal to the characteristic mixing length shared by the exchanging segments (cross-sectional area for horizontal exchanges, or surface area for vertical exchanges). The actual dispersive exchange between segments *i* and *j* at time *t* is given by:

$$\frac{\partial M_{ik}}{\partial t} = \frac{E_{ij}(t)A_{ij}}{L_{cij}} (C_{jk} - C_{ik}) \quad (\text{A.8})$$

where:

M_{ik} = mass of pollutant "k" in segment "i", in grams.

C_{ik}, C_{jk} = concentration of pollutant k in segment "i" and "j" in mg/l.

$E_{ij}(t)$ = dispersion coefficient time function for exchange "ij", in m^2/s .

A_{ij} = Interface area shared by segments "i" and "j", in m^2 .

L_{cij} = Characteristic mixing length between segments "i" and "j", in meters.

A.6. Boundary Processes

A boundary segment is characterized by water exchanges from outside the network, including tributary inflows, downstream outflows, and open water dispersive exchanges. WASP8 determines its boundary segments by examining the advective and dispersive segment pairs specified by the user. If an advective or dispersive segment pair includes segment number "0," the other segment number is a boundary segment. Thus, for advective flows, the segment pair (0,1) denotes segment 1 as an upstream boundary segment; segment pair (5,0) denotes segment 5 as a downstream boundary segment.

Boundary concentrations C_{Bik} (mg/L) must be specified for each simulated variable "k" at each boundary segment "i". These concentrations may vary in time. At upstream boundary segments, WASP8 applies the following mass loading rates:

$$V_i S_{Bik} = Q_{0i}(t) \cdot C_{Bik} \quad (A.9)$$

where:

S_{Bik} = boundary loading rate response of chemical "k" in segment "i," in g/m^3 -day.

V_i = volume of boundary segment "i," m^3 .

$Q_{0i}(t)$ = upstream inflow into boundary segment "i," m^3/day .

At downstream boundary segments, WASP8 applies the following mass loading rates:

$$V_i S_{Bik} = Q_{i0}(t) \cdot C_{ik} \quad (A.10)$$

where:

$Q_{i0}(t)$ = downstream outflow from boundary segment "i," m^3/day .

C_{ik} = internal concentration of chemical "k" in segment "i," mg/L.

Notice that the specified boundary concentration is not used to calculate the boundary loading rate for the downstream boundary segment. At exchange boundary segments, WASP8 applies the following mass loading rates:

$$V_i S_{Bi} = \frac{E_{i0}(t) A_{i0}}{L_{ci0}} (C_{Bk} - C_{ik}) \quad (\text{A.11})$$

where terms are as defined above. When a boundary concentration exceeds the internal concentration, mass is added to the boundary segment; when the boundary concentration falls below the internal concentration, mass is lost from the boundary segment.

A.7. Loading Processes

WASP8 allows the user to specify loading rates for each variable. Two types of loadings are provided for – point source loads and runoff loads. The first set of loads is specified by the user in the input dataset. The second set of loads is read by WASP8 from a nonpoint source loading file created by an appropriate loading model. Both kinds of loads, in kg/day, are added to the designated segments at the following rates:

$$V_i S_{Lik} = 1000 \cdot L_{ik}(t) \quad (\text{A.12})$$

where:

S_{Lik} = loading rate response of chemical "k" in segment "i," in g/m³-day.

$L_{ik}(t)$ = loading rate of chemical "k" into segment "i," kg/day.

A.8. Solids Transport

Solids Option 0 is chosen for a Solid system, then WASP8 will apply segment-specific settling and resuspension velocities as specified in the Parameter Data section, Solids group. This option is only descriptive and does not include process-based solids transport options. Settling is the movement of a solid from a water column segment to the underlying water column segment. Resuspension is the transfer of a solid from a surface benthic segment to the overlying water column segment.

The Descriptive Solids Transport (Figure A.1.A) option uses constant settling and resuspension velocities, which do not change with stream velocity. For this option, the settling velocity, v_s [m/s], and resuspension velocity, v_r [m/s], are entered for each solid type for each segment. As part of the model domain set up in the segment definition, the user enters which segment is below a given segment. WASP8 then knows, for a given segment, where both settling and resuspension are going to and coming from. Therefore, if a model has sand, silt, and clay, the settling and resuspension velocities for descriptive transport are determined by the user and entered directly into the interface.

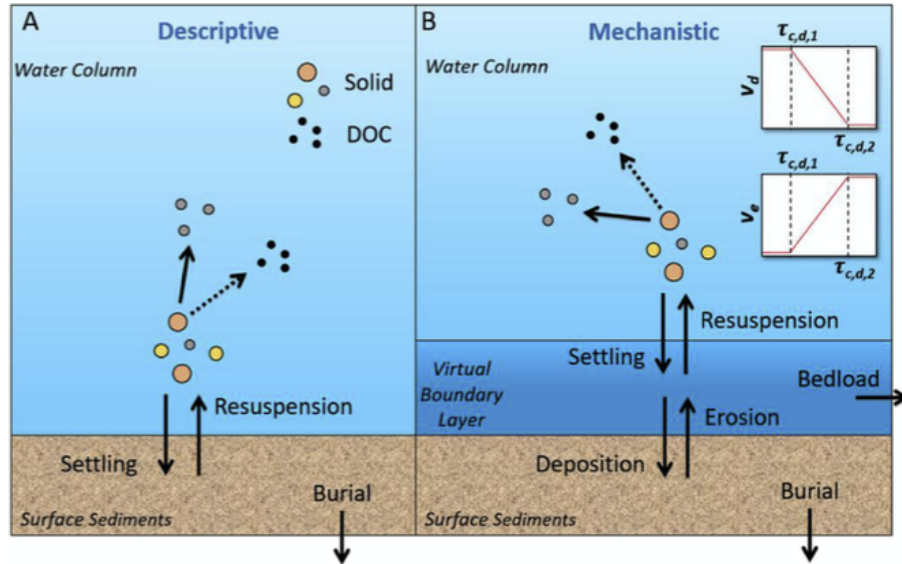


Figure A.1: Overview of processes for simulating solids in WASP8. (A) Descriptive and (B) Mechanistic. Source: Knightes et al. (2019).

A.9. Transport of pollutants or chemical tracers

The Advanced Toxicant module works with state variable classes (e.g., solute chemicals, nanoparticles, solids). By defining and parameterizing governing processes, the user effectively defines that state variable. Each state variable and process has different options for how it is described. Governing equations for concentrations follow the advection-dispersion-reaction equation. The science module and the transport module are solved using differential mass balance equations for each segment for each time step. The user may select different solution techniques, but generally, the forward Euler numerical approximation approach is used with varying time steps designed to minimize numerical instability.

Appendix B

Calculations performed and data model inputs

B.1. Dispersion coefficients

Table B.1: Hydraulic parameters and dispersion coefficients for each month (April to September 2004) and for each segment.

Segment	Width (m)	Depth (m)	Hydraulic radius (m)	Velocity (m/s)	Shear vel	D_L	Width (m)	Depth (m)	Hydraulic radius (m)	Velocity (m/s)	Shear vel	D_L
April 2004							May 2004					
1	47.115	1.14	1.1	0.815	0.088	161.79	42.185	0.895	0.865	0.765	0.086	148.99
2	48.35	1.455	1.405	0.63	0.065	107.49	43.615	1.215	1.175	0.59	0.063	95.22
3	21.465	1.705	1.605	0.925	0.094	27.14	20.55	1.44	1.365	0.835	0.087	25.88
4	20.925	1.935	1.795	0.855	0.085	21.40	20.155	1.665	1.56	0.76	0.077	20.04
5	22.97	2.07	1.94	0.715	0.070	20.42	22.255	1.785	1.69	0.625	0.063	18.99
6	23.34	1.865	1.745	0.78	0.078	25.08	22.225	1.61	1.515	0.69	0.071	22.76
7	20.91	2.275	2.055	0.735	0.071	15.98	19.685	2.05	1.865	0.63	0.062	13.26
8	29.435	2.195	2.03	0.57	0.056	25.40	27.55	1.955	1.815	0.49	0.049	21.08
9	31.46	1.79	1.69	0.625	0.063	37.85	26.345	1.87	1.73	0.55	0.055	22.44
June 2004							July 2004					
1	43.365	0.955	0.925	0.785	0.087	153.11	43.965	0.985	0.955	0.79	0.087	154.37
2	44.765	1.275	1.235	0.61	0.065	99.65	45.345	1.3	1.26	0.615	0.065	101.44
3	20.785	1.505	1.425	0.87	0.090	26.58	20.9	1.535	1.45	0.88	0.091	26.73
4	20.36	1.73	1.615	0.795	0.080	20.70	20.46	1.76	1.645	0.805	0.081	20.87
5	22.455	1.855	1.75	0.655	0.065	19.61	22.545	1.89	1.785	0.665	0.066	19.76
6	22.375	1.69	1.585	0.72	0.073	23.11	22.445	1.725	1.62	0.73	0.074	23.18
7	19.86	2.12	1.925	0.665	0.065	13.85	19.945	2.15	1.955	0.675	0.066	14.01
8	27.985	2.015	1.875	0.52	0.051	22.52	28.195	2.045	1.905	0.53	0.052	23.02
9	26.815	1.925	1.785	0.58	0.058	23.94	27.04	1.95	1.81	0.59	0.059	24.51
August 2004							September 2004					
1	47.345	1.155	1.11	0.82	0.088	162.49	46.61	1.12	1.08	0.815	0.088	160.68
2	48.57	1.465	1.415	0.65	0.067	111.28	47.88	1.43	1.385	0.635	0.066	107.85
3	21.505	1.72	1.615	0.955	0.097	27.91	21.38	1.675	1.58	0.925	0.094	27.34
4	20.97	1.95	1.805	0.88	0.087	21.97	20.85	1.905	1.77	0.855	0.085	21.53
5	23.015	2.085	1.95	0.735	0.072	20.94	22.905	2.04	1.915	0.715	0.070	20.56
6	23.415	1.885	1.755	0.8	0.080	25.64	23.17	1.85	1.725	0.775	0.078	24.71
7	20.995	2.29	2.07	0.75	0.073	16.35	20.73	2.26	2.04	0.725	0.071	15.58
8	29.71	2.205	2.045	0.58	0.056	26.25	29.105	2.175	2.015	0.565	0.055	24.82
9	31.79	1.805	1.705	0.64	0.064	39.30	31.07	1.775	1.68	0.625	0.063	37.19

B.2. Meteorological data

Table B.2: Example of input time functions for WASP model.

Date/Time	Solar radiation [W/m ²]	Wind speed [m/s]	Date/Time	Solar radiation [W/m ²]	Wind speed [m/s]
4/1/2004 0:00	0	1.72	4/2/2004 0:00	0	1.17
4/1/2004 1:00	0	1.83	4/2/2004 1:00	0	0.87
4/1/2004 2:00	0	1.58	4/2/2004 2:00	0	0.86
4/1/2004 3:00	0	1.53	4/2/2004 3:00	0	0.6
4/1/2004 4:00	0	1.61	4/2/2004 4:00	0	0.85
4/1/2004 5:00	0	1.23	4/2/2004 5:00	0	0.75
4/1/2004 6:00	0	1.17	4/2/2004 6:00	0	0.61
4/1/2004 7:00	0	1.49	4/2/2004 7:00	0	0.78
4/1/2004 8:00	7.19	0.69	4/2/2004 8:00	708.1	0.61
4/1/2004 9:00	8.69	0.74	4/2/2004 9:00	863.21	0.8
4/1/2004 10:00	9.31	1.16	4/2/2004 10:00	929.74	0.96
4/1/2004 11:00	9.63	1.89	4/2/2004 11:00	963.7	1.54
4/1/2004 12:00	9.78	2.83	4/2/2004 12:00	977.74	2.51
4/1/2004 13:00	9.78	3.49	4/2/2004 13:00	979.47	3.1
4/1/2004 14:00	9.67	3.97	4/2/2004 14:00	969.74	3.61
4/1/2004 15:00	9.42	4.52	4/2/2004 15:00	944.33	4.5
4/1/2004 16:00	8.93	4.44	4/2/2004 16:00	896.7	4.48
4/1/2004 17:00	7.97	3.79	4/2/2004 17:00	800.28	3.91
4/1/2004 18:00	0	3.19	4/2/2004 18:00	0	3.12
4/1/2004 19:00	0	2.72	4/2/2004 19:00	0	2.73
4/1/2004 20:00	0	2.01	4/2/2004 20:00	0	1.96
4/1/2004 21:00	0	1.56	4/2/2004 21:00	0	1.83
4/1/2004 22:00	0	1.26	4/2/2004 22:00	0	1.66
4/1/2004 23:00	0	1.32	4/2/2004 23:00	0	1.7

Appendix C

Bootstrap PAHs concentrations

C.1. Naphthalene

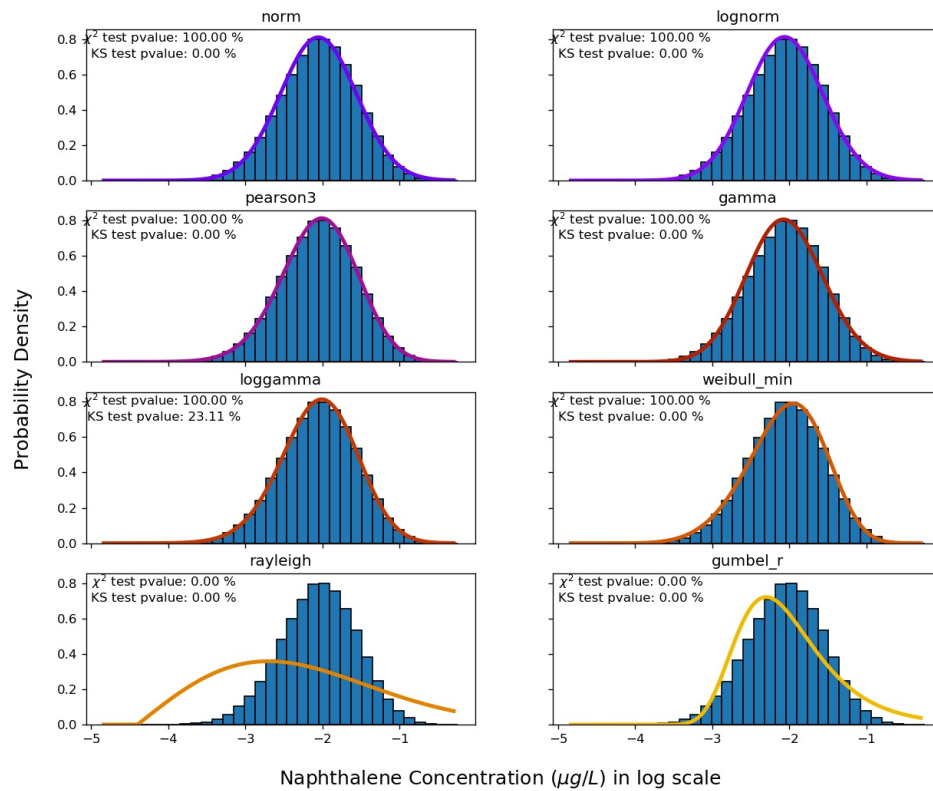


Figure C.1: Probability distribution function for Naphthalene

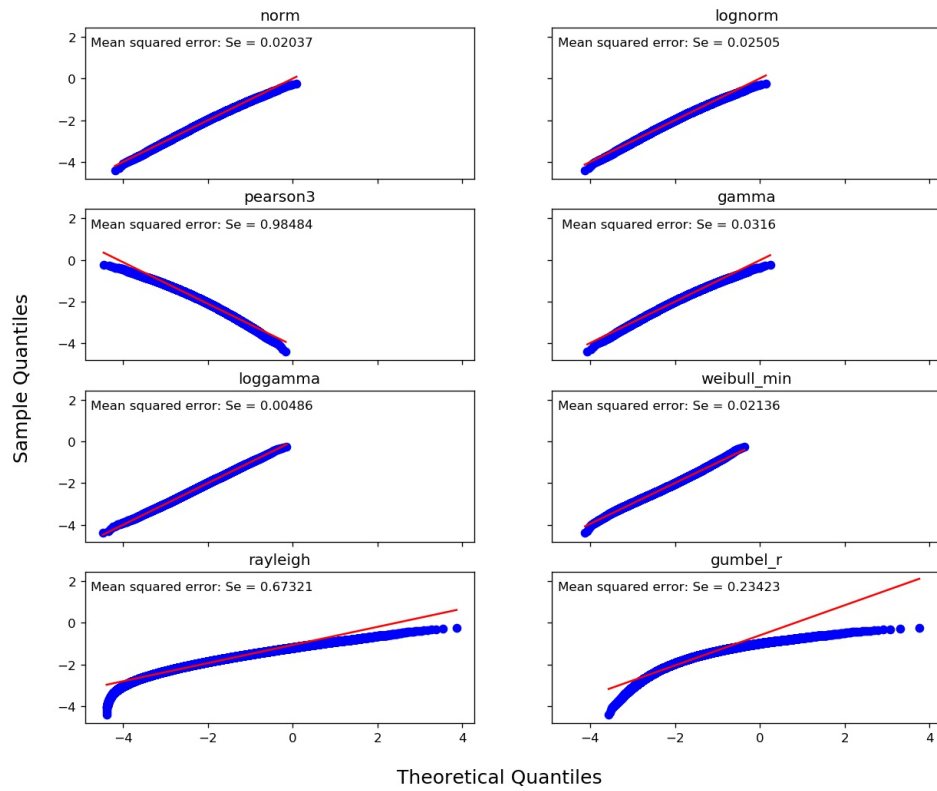


Figure C.2: Q-Q plot for Naphthalene

C.2. Benzo[a]pyrene

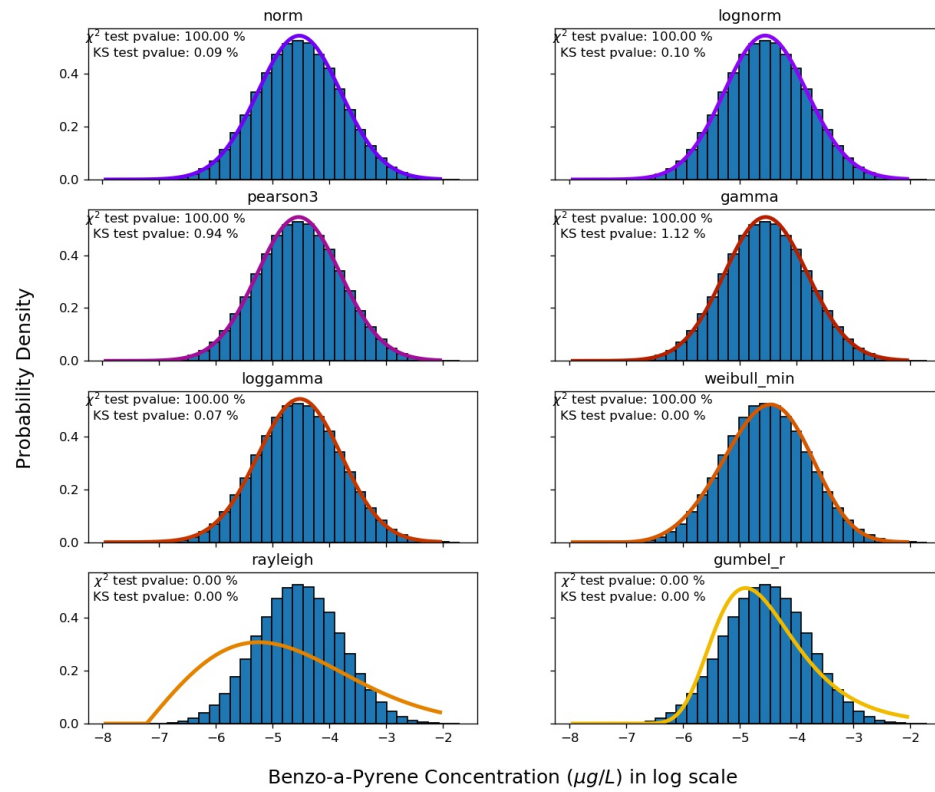


Figure C.3: Probability distribution function for Benzo(a)pyrene

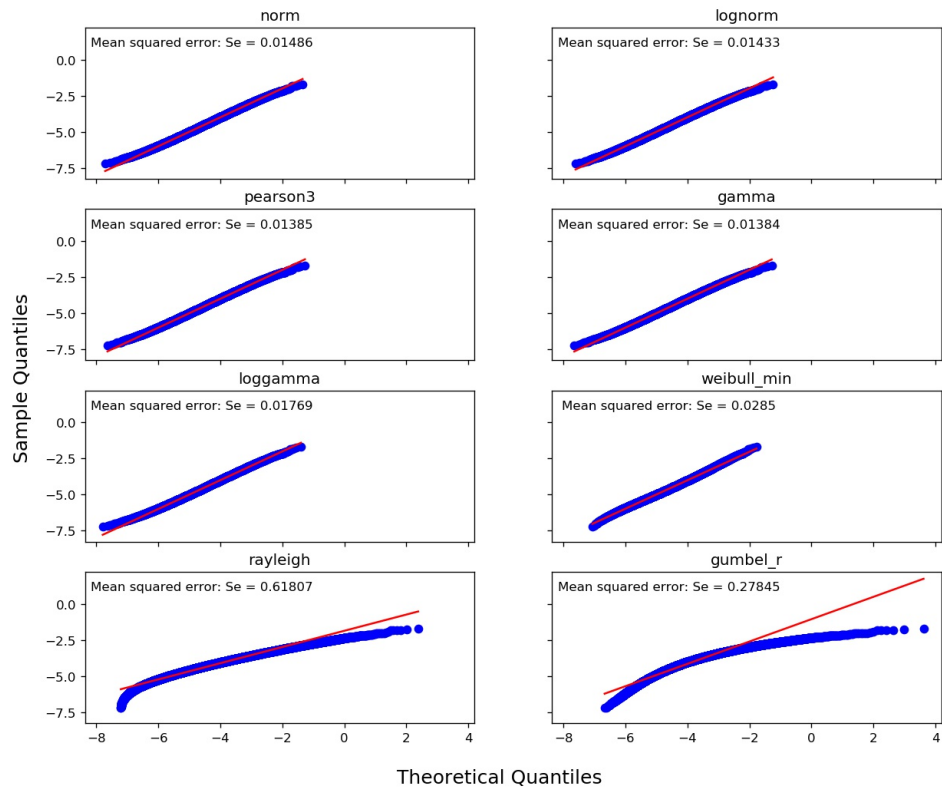


Figure C.4: Q-Q plot for Benzo(a)pyrene

Appendix D

Study zone photographs



Figure D.1: La Farfana WWTP discharge zone.